Flood Analysis of a Water System after Failure of a Spill-Lock Complex

Case Study:
Spill-Lock Complex IJmuiden

Civil Engineering

Lennard Zeelenberg

TU Delft

Flood Analysis of a Water System after Failure of a Spill-Lock Complex

Case Study: Spill-Lock Complex IJmuiden

by

Lennard Zeelenberg

In partial fulfillment of the requirements for the degree of,

Master of Science

in Civil Engineering

at the Delft University of Technology,

to be publicly defended on Wednesday 7 May 2025, at 15:00

Student Number:	4872258
Thesis committee:	Dr. M. Pregnolato (chair)
	L. van Gijzen MSc (daily supervisor)
	Dr. Ir. A.M.R. Bakker
	Dr. Ir. O.A.C. Hoes
Faculty:	Faculty of Civil Engineering and Geosciences, Delft
Department:	Hydraulic Engineering
Specialization:	Hydraulic Structures and Flood Risk

TU Delft

Preface

This thesis concludes the master Hydraulic Engineering at the Technical University of Delft. I really enjoyed working on a real life case study, provided by Rijkswaterstaat. Due to the event on the 2nd of November 2023, the topic is really up-to-date, which makes the research relevant. The biggest lesson that I have learned during this process is creating a hydraulic model of an existing water system with the HEC-RAS software. Especially with the feedback of one of my supervisors, Olivier Hoes, the model was set up for which I would like to express my gratitude.

I would also like to thank Maria Pregnolato for chairing my graduation committee and the feedback that I received during the progress meetings. Additionally, I would like to thank my supervisor Alexander Bakker for the feedback sessions and support from Rijkswaterstaat. I would also like to thank my daily supervisor, Laurie van Gijzen, for all the weekly sessions and useful discussions on the contents. Your guidance really supported this research and the process towards the end result.

At this moment I am looking back on a very interesting Master at the Delft University, and at the same time, I am looking forward to the coming chapters in my career. I am thankful that I had the opportunity to perform my bachelor and master at the TU Delft. The knowledge obtained during my study will undoubtedly support me in the coming future.

Last but not least, I would like to thank my friends and family, for their support and confidence throughout all the years.

Lennard Zeelenberg
Rotterdam, May 2025

Summary

On the 2nd of November 2023 a storm event coincided with the non-closure of the spill gates in the spill-lock complex in IJmuiden. This resulted in serious water level rise on the water system due to inflow of sea water. The margins for the water levels in the fully closed water system are very tight. In the end the failure was identified and the appropriate measures where taken to prevent larger damage. This incident revealed that not only the discharge capacity of the pumps and spill could result in significant water level increase, but also failure of retaining sea water results in such water level rise. This research was set up to study the behavior of the high water in the water system, with the focus on the two main canals, the North Sea Canal and Amsterdam Rhine Canal.

With the use of a probabilistic analysis, the most relevant failure scenarios are selected to use in a model simulation. With additional literature and the use of event trees the probabilistic analysis was performed for the failure mechanisms overtopping and non-closure for the spill and ship locks separately. The probabilistic analysis revealed that only non-closure of the spill gates and outer heads of the ship locks where relevant failure mechanisms based on the return period of the events.

Using the software of HEC-RAS a two-dimensional model was developed to resemble the North Sea Canal and Amsterdam Rhine Canal, together with the spill-lock complex in IJmuiden. Calibration of the model was performed using measured data obtained throughout the canals, during the failure event on the 2nd of November 2023. After calibration, the relevant failure scenarios were provided for the model, resulting in the flood wave behavior through the system. The ship lock failure resulted in acceptable high water scenarios, as an extreme event was modeled to test the impact of such failure.

In the end only non-closure failure of the spill gates was modeled in detail to determine the risk of flooding. The duration of the opened spill gates was selected to be 6 hours, as 3 hours of failure needed more variation in storm duration, whereas the storm duration in this research was taken as a constant. Furthermore, 12 hours of opening of all spill gates was deemed to be highly unlikely, as all spill gates are able to be closed manually with the use of gravity. In the end, the effects of the high water scenarios were needed to determine the final flood risk. Although the effect calculation is only based on a rough estimate, it gives an idea of the scale of the effects.

All relevant failure scenarios with their defined probability of occurrence where calculated with the model, resulting in the maximum high water levels per scenario. This maximum water level was coupled to the estimated cost of damage. The probability of occurrence together with the estimated cost of damage resulted in a risk for every scenario. Finally, the total final risk for 6 hours of non-closure of all spill gates in IJmuiden was computed.

Contents

Preface ii

Summary iii

Nomenclature vi

1 Introduction 2
- 1.1 Research Context . . . 2
- 1.2 Research Problem . . . 2
  - 1.2.1 Literature Review . . . 3
- 1.3 Research Objectives . . . 3
- 1.4 Research Scope . . . 4
- 1.5 Research Questions . . . 5
- 1.6 Research Approach . . . 5

2 Case Study: IJmuiden 8
- 2.1 Geographical Context . . . 8
- 2.2 Historical Background . . . 11
  - 2.2.1 Water System NSC and ARC . . . 11
  - 2.2.2 Complex of IJmuiden . . . 11
- 2.3 Dimensions . . . 11
- 2.4 Locking Process . . . 12
- 2.5 Bathymetry . . . 13

3 Failure Mechanisms 14
- 3.1 Ship lock failure . . . 14
  - 3.1.1 Probabilistic Approach . . . 15
  - 3.1.2 Storm Scenario for Non-Closure of the Outer Head of the Middensluis . . . 17
- 3.2 Spill failure . . . 17
  - 3.2.1 Probabilistic Approach . . . 18
  - 3.2.2 Storm Scenarios for Non-closure of the Spill . . . 18

4 Model 22
- 4.1 Model Configuration . . . 22
- 4.2 Model Calibration . . . 23
  - 4.2.1 Computational Time Interval . . . 23
  - 4.2.2 Equation Set . . . 24
  - 4.2.3 Pump Behavior . . . 26
- 4.3 Model Validation . . . 27
- 4.4 Model Simulations . . . 27
  - 4.4.1 Model Runs Non-Closure Middensluis . . . 27
  - 4.4.2 Model Runs Non-Closure Spill . . . 29
  - 4.4.3 Flood Wave Behavior . . . 32

5 Effects 34
- 5.1 Water System . . . 34
  - 5.1.1 Main Canals . . . 34
  - 5.1.2 Main Side Rivers . . . 35
  - 5.1.3 Polders . . . 36
  - 5.1.4 Additional Damages . . . 36
- 5.2 Critical Flood Locations . . . 36
- 5.3 Economical Effect . . . 36

6 Discussion **42**
6.1 Difference between Spill and Ship Lock Failure 42
6.2 Duration of Spill Failure 43
6.3 Review Legal Assessment 43
6.4 Limitations 44

7 Conclusion and Recommendations **46**
7.1 Conclusion 46
7.2 Recommendations 47

References **49**

A Research Path **51**

B Water Boards in the System **53**

C Geographical Background of the Water System **54**

D Bathymetry NSC and ARC **58**

E Event Trees **61**

F Model Results **64**

G 6h Failure Runs **69**

H Critical Flood Locations **76**
H.1 Height Maps 77
H.2 Damage Cost of Flooding 79

Nomenclature

Abbreviations

Abbreviation	Meaning
ARC	Amsterdam Rhine Canal
DWE	Diffusion Wave Equations
DWTP	Drinking Water Treatment Plant
GPD	Generalized Pareto Distribution
HVS	Haringvliet Spills
IH	Inner Head
NAP	Normaal Amsterdams Peil
NSC	North Sea Canal
OH	Outer Head
SSM	Damage and casualties module (Dutch: Schade Slachtoffer Module)
SWE	Shallow Water Equations

1

Introduction

1.1. Research Context

Storm *Ciarán* reached the Netherlands on the 2nd of November 2023, it coincided with the non-closure of the spill gates at the spill-lock complex in IJmuiden. As a consequence of this event, the water levels on both the North Sea Canal (NSC) and Amsterdam Rhine Canal (ARC) began to rise. The elevated water exceeded several critical values, meaning action had to be taken to prevent the flooding of cellars and sewage systems, for example in Amsterdam. In the end, the appropriate measures were taken and the malfunctioning spill gates were closed manually. The close escape of a flooding was a reason to study failure events similar to the event on the 2nd of November 2023. In particular, the event demonstrated the need to connect failing of the spill-lock complex, such as the incident on November 2nd, to the flood risk of the water system.

1.2. Research Problem

High water levels on the canals form an increased flood risk for the (populated) areas connected to the water system. Flooding of the water system can be caused by two failure mechanisms, both associated with the spill-lock complex located at the connection between the canal and the sea. The water level at the canal rises when the inflow exceeds the outflow. When the discharge capacities of the pumping station and spill at the complex of IJmuiden are not sufficient to discharge the excess water from the water system and its polders, water rises on the canal. Failure of retaining sea water by the spill-lock complex is the second failure mechanism, leading to an increased inflow into the water system. Failure of retaining high water at sea can be caused by overtopping of the retaining structures or non-closure of the movable gates of the spill or ship locks.

Existing research performed for Rijkswaterstaat focuses mainly on the first mentioned failure cause, concerning the ability of discharging fresh water from the NSC into the North Sea (Rijkswaterstaat, 2014; Kuijper and Geerse, 2016; Zethof et al., 2023). The spill-lock complex of IJmuiden is periodically assessed on its safety against flooding from the sea, as it is one of the critical components of the Dutch coastal defense infrastructure (Van den Berg et al., 2019). These assessments are mandatory according to the Dutch Water Act and are reported to the Ministry of Infrastructure and Water Management of the Dutch Government (Water Act, 2025).

In the most recent legal assessment of the sea water retaining capabilities of the spill-lock complex, the failure mechanism of non-closure of the spill gates is considered to be negligible (Van den Berg et al., 2019). This conclusion was based on a probabilistic analysis, resulting in very low likelihood of occurrence of such an event. However, the described failure event on the 2nd of November demonstrates that this failure mechanism can not be neglected. A closing failure of the spill gates did increase the water level on the NSC and ARC and caused nuisances to the surroundings of the water system.

In the legal assessment, failure of the water system is defined as the probability that the incoming

volume of sea water exceeds the total storage volume of the system, described by the following formula:

$$P_{flooding} = P(V_{in} > V_{Storage}) \tag{1.1}$$

This comparison of the volumes does not take into account that the incoming water moves through the system as a flood wave, seeking an equal distribution of mass over the entire water system. There is a knowledge gap on the behavior of such a flood wave through the system. Furthermore, different failure scenarios result in different water volumes entering the water system. The different possible failure scenarios are to be coupled to the flood risk of the water system and its surroundings.

1.2.1. Literature Review

Research on high water retaining components of a water system, similar to the water system in IJmuiden, is conducted for various structures, such as canal levees and (flood)gates. An analysis of existing literature results in methods to assess flooding of canal levees. A Dutch program is set up for the assessment of flooding of delta levees in the Netherlands (Jongejan and Maaskant, 2013). Another research obtains to expand the knowledge for the determination of failure probabilities for canal levees (Lendering et al., 2018). Triki (2017) describes the effects of resonance of free-surface waves generated by for example, opening or closure of spill gates. The increasing magnitude of such free-surface waves can lead to dangerous overtopping of the canal levees in case the wave oscillation matches one of the natural oscillations of the canal (Triki, 2017). Another research is conducted on the difference between free flow and submerged flow for spill structures (Salmasi and Abraham, 2023).

Research on a similar structure as the spill-lock complex IJmuiden is found for the storm surge Maeslantbarrier in Rotterdam. The Maeslantbarrier also protects a long canal against high water from the same North Sea. In the research a probabilistic method is presented to relate failure of a storm surge barrier to the exceedance frequencies of the water levels in the canal behind the barrier (Mooyaart et al., 2025). In relation to this research, there is also research on the economical optimizations for coastal flood defense systems with regards to the improvement of closure reliability and the raising of flood defenses behind the barrier (Mooyaart et al., 2023). However, the main distinction is that the barrier in IJmuiden was not constructed solely to withstand high water, whereas the storm surge barrier is built for this purpose. Another difference is that the spill gates in IJmuiden are closed more frequent, whereas the considered storm surge barrier is only closed in case of expected large storm events with an expected sea water level above +3.0 m NAP. The storm surge barrier blocks the whole canal with two floating doors, while the spill-lock complex still provides a shipping connection by means of the locks as long as the water level difference does not reach the operational limit for the ship locks.

There is a lot of research available on dam brake flood waves. Dam brakes release a significant volume of water onto the canal in downstream direction, that creates a flood wave through the water system. In this sense, there are similarities with failure of the spill-lock complex. However, with dam break failure a large volume is released at a sudden, while for failure of the spill-lock complex, water flows in more gradual and most of the time with smaller volumes. Next to that, the water propagates downstream for dam break flow, and upstream for spill-lock failure. There is research available that describes the modeling of a dam break induced flow, where the shallow water approach is compared to fully three-dimensional simulations (Biscarini et al., 2010). Another research discusses the methodologies used in other studies to describe the propagation of a dam break flood wave (Peramuna et al., 2024). Also the form of the canal is varied to see the effect on the flood wave propagation (Wang et al., 2019).

Although the mentioned research all show some similarities with failure of a spill-lock complex. Failure of such a complex and the consequences for the water system are not researched. As well as the manner of failure. This research is targeted to find an answer for these knowledge gaps. This research focuses on the complex in IJmuiden as being the case study, where the main canals and side rivers form the water system.

1.3. Research Objectives

This research aims to analyze the behavior of incoming sea water moving through the water system due to failure of a spill-lock complex. The research is conducted as a case study with the spill-lock complex of IJmuiden separating the North Sea from the protected water system. In contrast to existing literature, this research examines the inflow of sea water into the North Sea Canal and Amsterdam

Rhine Canal. This research also provides insights in the behavior of the high water in the system and sets up a starting point to link high water in the canal to effects regarding flood damage. In general this research provides an insight in how the water system behaves and reacts to certain failure. This kind of information is useful for the maintenance and renovation strategy of the complete system in the future. As well as the strategy during failure and high water on the canal.

1.4. Research Scope

This research focuses on the flood risk of the water system due to failure of the spill-lock complex IJmuiden, which causes inflow of sea water in the system. The focus lies on the increase of water level in the canal solely as a result of inflowing sea water. High water in the canal resulting from an insufficient discharge capacity of the pumps and spill in IJmuiden is not considered in this research. Malfunctioning of the spill-lock complex in the context of this research does not mean that the spill and locks are not performing as intended, however that the spill and locks are unable to retain (high) water at sea.

Sea water cannot flow from the sea into the canal via the pumping station, as the pump tubes are watertight in this direction by means of check valves. Therefore, this research only focuses on the failure of retaining the sea water from the spill and the ship locks present in the complex.

The water system consists of the North Sea Canal and the Amsterdam Rhine Canal. Major inflow from the polders during failure and high water at the canal is not taken into account. During failure there is a continuous communication between Rijkswaterstaat and the water boards responsible for the polders. The polders depend on the canals for their discharge of excess water. During critical high water at the NSC and ARC, pumping from the polders is regulated and in case the water levels get critical, a full pumping stop can be ordered by Rijkswaterstaat.

The salt barrier that is built at this moment in IJmuiden is not considered to be of major influence on the behavior of the flood wave. The salt barrier is located behind the spill and has a minimal influence on the amount of sea water entering the system. Also the sea water retaining ability of the spill-lock complex is not influenced by the salt barrier, at most the sea water will be obstructed while moving through the spill canal. Research on the full effects of the salt barrier on the water system should prove whether these assumptions can be made or if the salt barrier should be included in the research.

Failure of the spill-lock complex is possible due to a variety of failure causes (Lewin et al., 2003). Failure of retaining the sea water by the retaining structures in the complex is possible in the form of the following four failure mechanisms: non-closure failure, overtopping failure, piping failure and failure of (structural) strength (t' Hart, 2018). The focus of this research lies on the failure mechanisms: non-closure and overtopping. The failure mechanism piping is expected to be sufficiently prevented by the seepage screens that are present for the structures in the system. The failure mechanism structural failure is also not taken into account, as the focus of this research is not on the structural analysis of the complex.

1.5. Research Questions

The research questions and sub-questions, forming the basis of this research, are presented in the following section. The main research question is:

What is the increased flood risk on the water system, North Sea Canal and Amsterdam Rhine Canal, as a result of inflowing sea water due to overtopping and non-closure failure of the spill-lock complex IJmuiden?

The main research question is answered with the use of the following sub-questions:

1. **What are the relevant failure scenarios for the spill-lock complex, leading to entering of sea water into the water system?**
   First the relevant failure mechanisms and scenarios are to be determined to narrow the focus of this research and to filter out the irrelevant and unlikely failure scenarios. The failure scenarios induce an inflow of sea water into the system, creating the flood wave. It is necessary to determine the probability of occurrence per failure scenario. With the use of the probabilities, the most critical failure events are selected to examine their effects.
2. **How does a flood wave evolve through the water system behind the spill-lock complex in IJmuiden?**
   To determine the behavior of the flood wave through the water system, a model is set up. The model needs to run different scenarios for the different types of failure. The model needs to demonstrate the flood wave behavior as it propagates through the system, and return the water levels at several critical locations in the water system. The selection at the first sub-question is used to model the relevant failure scenarios. The most critical failure scenario is worked out in detail, with the use of the model. With the behavior of the flood wave, the failure of the spill-lock complex can be related to the flood risk of the water system.
3. **What are the consequences of the failure scenarios, due to their induced flood wave on the water system?**
   The different high water scenarios for the water system need to be related to the consequences as a result of for example (local) flooding. The consequences together with the probability of occurrences results in a flood risk for the water system. The consequences are expressed as an economical value, describing the cost of damage of a certain water level in the canal.

1.6. Research Approach

This section explains the approach and methods used to answer the different research (sub)questions. The research path is presented in Figure 1.1 and schematically presents the approach of the research. An enlarged version of the research path can be found in Appendix A.

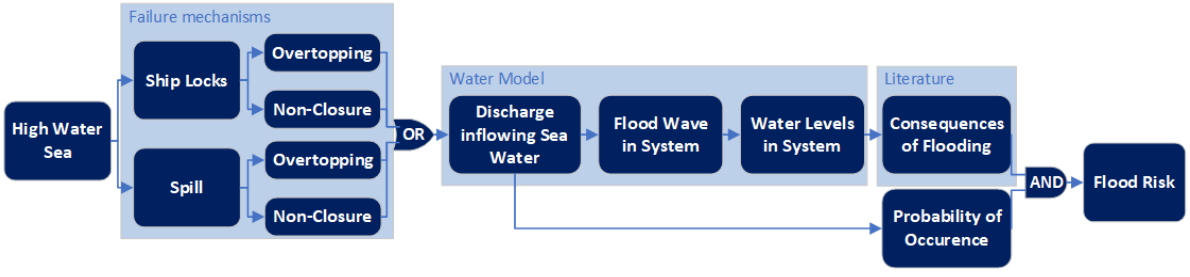

Figure 1.1: Research path

Chapter 2 gives geographic and historic background concerning the case study area, as well as useful information about the components in the system.

Chapter 3 compares the existing failure scenarios for overtopping and non-closure of the ship locks and the spill. After the determination of the return periods for the events, the relevant failure events are filtered and used in the further analysis with the model. The probabilities of occurrence are derived with use of results obtained from literature review, existing data from Rijkswaterstaat and the use of

event trees as described by Hill et al. (2002). The probability for overtopping of the retaining structures is related to the return periods of certain extreme water levels at the North Sea (Chbab, 2017). The probability for non-closure of the ship locks is derived with the use of event trees. For the probability of non-closure of the spill, available probabilistic analysis for the Haringvliet Spills is used to compare with the spill at IJmuiden. For the storm generation of the extreme storms overtopping the retaining structures, a storm surge generator is used (Bakker et al., 2025). Lower storms are generated similarly for failure of non-closure of the spill. Chapter 3, formulates an answer for the first sub-question.

The second sub-question is answered with a combination of a literature review and the assistance of modeling software. The modeling software is intended to describe the water behavior and movement through the water system. Input for the model are the results of sub-question 1 in the form of scenarios to run through the model. The modeling software that is used is the HEC-RAS(6.6) modeling software, where 2D unsteady flow analysis is performed for the water system. Chapter 4 presents the setup of the model. The model is calibrated visually according the measured data from the failure event at 2 November 2023. Validation of the model is a more difficult task, as there is only one failure event. In the end of Chapter 4 the model runs are presented for the selected failure scenarios. After the analysis of the results, the most critical failure scenario is selected and worked out in further detail.

The third sub-question is answered with the use of available literature, as high water on the water system needs to be coupled to damages. The results from the second sub-question will be used as information to estimate the damage to the water system. This analysis can be found in Chapter 5. The combination of the probabilities of occurrence of a certain failure scenario with the corresponding damages, will lead to the total flood risk of the water system. Finally, the answers to all sub-question will form the answer on the main research question.

2

Case Study: IJmuiden

This chapter describes the geographical context and historical background for the water system and spill-lock complex in IJmuiden. This research is based on a case study of the spill-lock complex in IJmuiden.

2.1. Geographical Context

The water system examined in this research consists of two main canals, the North Sea Canal (NSC) and the Amsterdam Rhine Canal (ARC). Numerous side canals and basins are attached to the main canals. The water system is a fully closed hydraulic system by means of (ship) locks. The full closed water system contains in total 51 ship locks of varying sizes. The ARC is hydraulically closed at Wijk bij Duurstede in the south by the Prinses Irene Locks and hydraulically closed from the Lek river by the Prinses Beatrix Locks. At Zeeburg (Amsterdam), the ARC continues as the NSC westward towards IJmuiden. The Oranje Locks form a closed connection between the Markermeer and the NSC. At IJmuiden the spill-lock complex separates the system from the North Sea.

The major side rivers are the Amstel, from the south towards Amsterdam and the Vecht from Utrecht towards the Markermeer. The Amstel is further divided in several other tributaries along its stretch. The geographical positioning of the NSC, ARC, main side rivers and the biggest and most important locks are depicted in Figure 2.1 and enlarged visible in Appendix C. The total area of the complete water system is: 3906 ha (Van den Berg et al., 2019). During high water events, part of the system is disconnected and the total area of the water system decreases to 2700 ha.

Four water boards depend on the main canals to discharge excess water out of the surrounding polders, these water boards are visualized in Appendix Figure B.1. Excess water is discharged by 116 local pumping stations, all varying in size and spread throughout the water system. The locations of the pumping stations are also presented in Figure 2.1. A large part of western Netherlands relies on the water system to maintain acceptable water levels within the polders. The area of the whole drainage system is nearly 300 000 ha. In normal operation, the discharge of this extensive system towards the sea is provided by the pumps and spill located in IJmuiden. The availability of these pumps and spill is critical. If the pumps and spill are temporarily not available, the water needs to be stored within the water system and/or polders. Additionally, high precipitation events can result in a large amount of excess water to be discharged from the water system. Both situations lead to increased water levels in the water system. However, as already mentioned in Section 1.4 a lack of availability or capacity of the pumps and spill is not the focus of this research. The focus is on the sea water retaining ability of the spill-lock complex in IJmuiden.

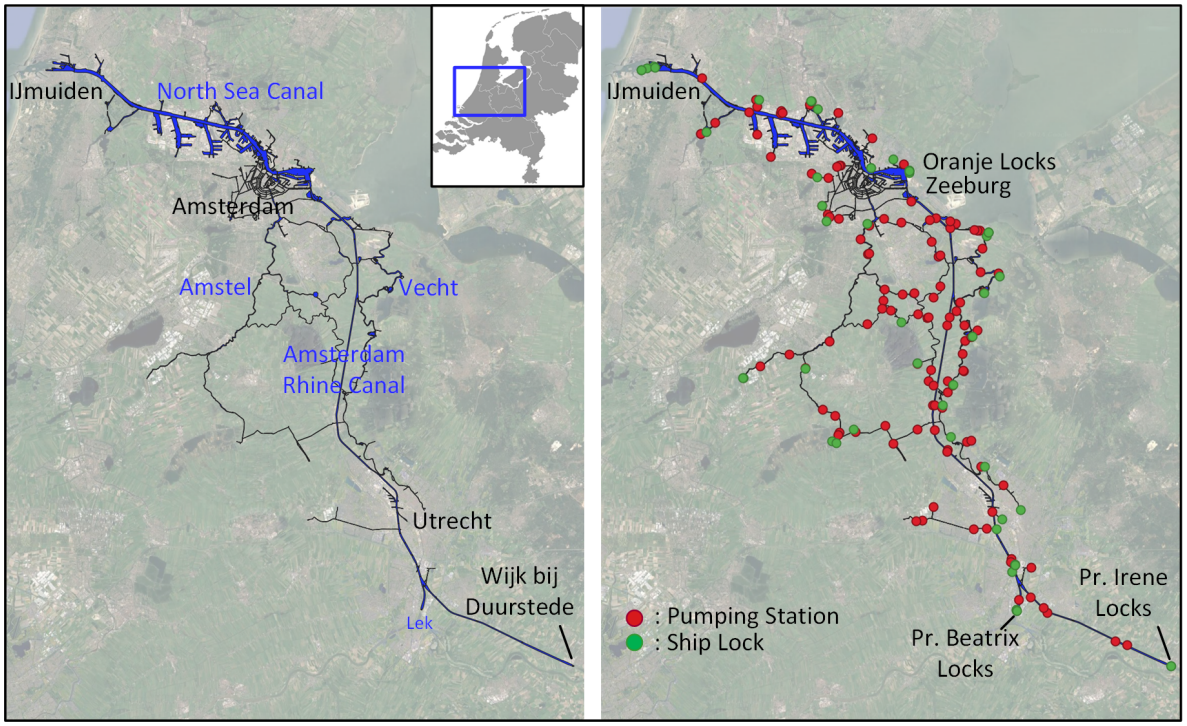

Figure 2.1: Geographic position of the water system (left) and the pumping station and ship lock locations (right)

The complex is part of dike trajectory 44-3, as visualized in Figure 2.2. The complex includes five ship locks, a spill and a pumping station, the latter two are important for the water level regulation on the canal. The ship locks in order of increasing size are named: Kleine Sluis, Zuidersluis, Middensluis, Noordersluis and Nieuwe Zeesluis. Ground masses are present in between the hydraulic structures. The system is enclosed by the elevated terrain of the Tata Steel factory on the north side and the city of IJmuiden on the south side. Figure 2.3 presents the position of all the different hydraulic structures located within the complex.

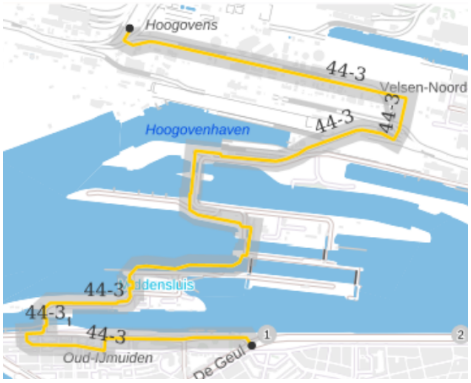

Figure 2.2: Dike trajectory 44-3

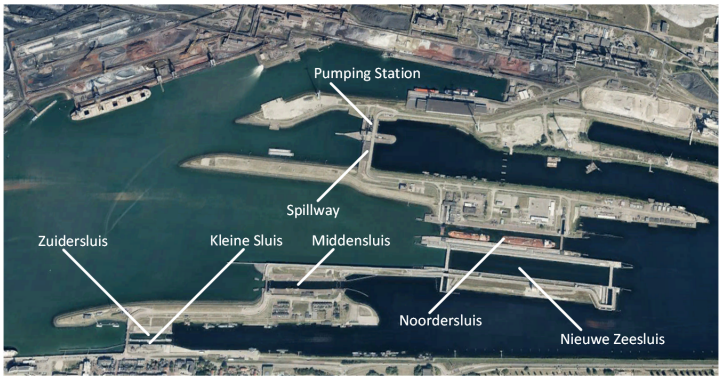

Figure 2.3: Components in the IJmuiden complex

The water balance of the NSC and ARC is schematically illustrated in Figure 2.4. Water enters and leaves the system via various water fluxes. The dominant inflow of water on the main canals is a result of the pumping of excess water out of the polders. This pumping is performed to maintain a certain water level in the low lying polders, the excess water is pumped out of the polder by local pumps. There are 116 local pumps distributed across the water system. The contribution of the local pumping station to the water levels at the canals is significant, but not in the scope of this research. With significant high water on the canal, Rijkswaterstaat orders the local water boards to limit or stop their pumping on the canal (Van Beekvelt et al., 2022). The locations of the pumping stations are visible in Appendix C.

Another water flux is the direct precipitation and evaporation of water from the canal surfaces, however the volumes of water from direct precipitation and evaporation are negligible compared to the dominant water flux. Similarly, due to the filling and leveling of the ship locks, a small amount of water is interchanged between the canal and the lock. This water flux is also of minor contribution in the total balance and is therefore considered negligible for the purpose of this research.

Water flow out of the system via the available pumping stations and the spill at IJmuiden. The largest pumping station is situated in IJmuiden, but also pumping station Zeeburg has a significant pumping discharge onto the Markermeer. Spilling at IJmuiden is preferred, as spilling requires the least amount of energy compared to pumping. Additionaly, the discharge capacity of the spill is higher than the pumps, but the spill is restricted to a limited window, where the sea level needs to be below the canal level. The schematic overview in Figure 2.4 only considers the water fluxes during normal conditions, it excludes water fluxes entering the system due to failure of the spill-lock complex in IJmuiden.

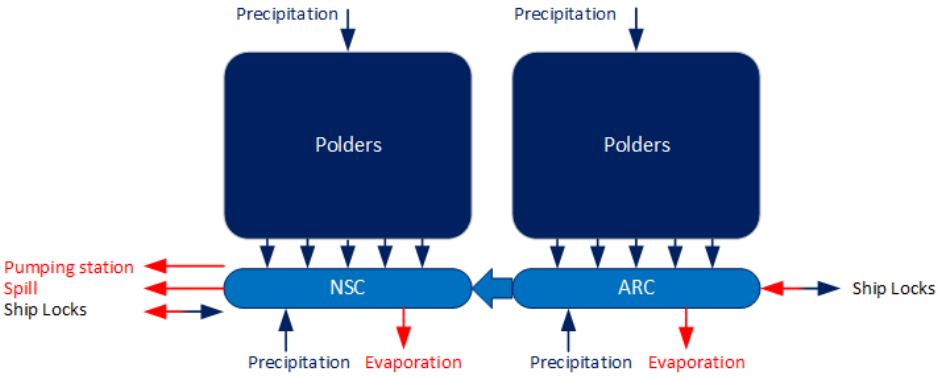

Figure 2.4: Schematic visualization of the NSC-ARC water balance (not to scale)

The water level on the canal needs to be maintained around its target level. When the water level on the canal rises, nuisance and eventually local flooding of the water system can be one of the outcomes. In contrast to the problems arising with high water, lower water levels are a problem for ships that need to navigate over canal structures under water, requiring a specific draft. The most used and important instrument to regulate the water level on the NSC-ARC system is the spill-lock complex in IJmuiden.

The water system has very tight margins to maintain with respect to the critical water levels. The target level in the water system is: -0.40 m NAP. The minimum desired water level of the canals is -0.55 m NAP. The first critical high water level is -0.30 m NAP, when this water level is exceeded, the request to limit the discharge on the NSC and ARC is send to the regional water boards. When the water level rises towards +0.00 m NAP, Rijkswaterstaat announces a full discharge stop on the NSC and ARC and the discharge of excess polder water on the canal is not allowed. All the procedures and agreements can be found in the *Waterakkoord* (Van Beekvelt et al., 2022), which prescribes the measures to be taken in case of high water. Table 2.1 illustrates the critical water levels on the North Sea Canal.

Water level (...m NAP)	**Characteristics**
> +0.00	Extreme high water
> -0.15	High water
> -0.25	Increased water level
> -0.30	Slightly increased water level
-0.40	Target level
< -0.55	Low water level

Table 2.1: Critical water levels on the North Sea Canal

Due to failure of preventing sea water entering the water system at the spill-lock complex IJmuiden, the water levels on the canal will be raised. Due to the tight margins for the water system, high water problems will arise in a relatively short time span. The sea water enters the system at IJmuiden and will gradually propagate in upstream direction through the water system in the form of a flood wave.

2.2. Historical Background

This section describes the historical background of the NSC and ARC and the background of the complex in IJmuiden. The historical progression is driven by the increasing sizes of ships as a result of industrial growth and improving ship building techniques.

2.2.1. Water System NSC and ARC

The Noordhollandsch canal was built in 1824 as an alternative route for the shallow ship route via the Zuiderzee. This canal connected the port of Amsterdam with Den Helder in the north. However, this canal quickly became to small for the increasing ship sizes. Therefore, the 21 kilometers long North Sea Canal was finished in 1876, providing a short connection between the port of Amsterdam and the North Sea. This lateral route was built through the dunes.

The 72 kilometers long Amsterdam Rhine Canal was a project of improving the Merwede Canal, which had existed since 1892. The Merwede Canal also became to small to function for the new sizes of ships. The ARC would improve the connection between Amsterdam and the German hinterland. At the North of Utrecht, the Merwede Canal was the basis for the current ARC, at the south of Utrecht the canal was newly dug. The project was started in 1931, during the crisis of the 1930s and the 2nd World War, therefore experiencing delays. Final completion of the ARC was in 1952.

2.2.2. Complex of IJmuiden

With the completion of the NSC, also the ship locks Kleine sluis and Zuidersluis where built. After 20 years, the Middensluis was built to provide passage for the bigger ships. The ever growing sizes of the ships resulted in the building of the Noordersluis, being the biggest ship lock in the world for that time. Recently, the Nieuwe Zeesluis carries the same title and provides service for the biggest ships in the world.

The spill was initially being built as an inlet, with the idea that it could be used to put land under water as a defense mechanism in times of wars. However, the construction was finished after the German invasion in World War II. After completion the inlet was used as a spill for discharging the canal to the sea and still functions this way. The spill was not always reliable enough to discharge all excess water, because spilling can only happen in case the sea water is lower than the canal level. In 1975 the pumping station was built to bring more discharge capacity and reliability.

2.3. Dimensions

The types of locks and relevant dimensions of the locks are given in Table 2.2. All locks share the same three functions: leveling the water system for passing ships between the North Sea and canal, protection against high water at sea and allowing road traffic to pass the canal. The dimensions of the spill and pumping station are given in Table 2.3. The three main functions of the pumping station and spill are: maintaining the water level on the water system NSC-ARC, protection against high water at sea and allowing road traffic to pass the canal.

	Year	Gate Type	Ret. height OH +... m NAP	Ret. height IH +... m NAP	Length [m]	Width [m]	Depth [m]
Kleine Sluis	1876	Mitre	4.85	3.50	120	12	3.75
Zuidersluis	1876	Mitre	4.85	3.50	120	18	7.85
Middensluis	1896	Mitre	5.85	2.50	225	25	10
Noordersluis	1929	Roller	5.85	3.40	400	50	15
Nieuwe Zeesluis	2022	Roller	8.85	8.85	500	70	18

Table 2.2: Dimensions locks

	Year	Ret. height +... m NAP	$Q_{out,max}$ [m^3/s]	# tubes
Spill	1945	7.00	900	7
Pumping Station	1975	9.00	260	6

Table 2.3: Dimensions spill and pumping station

The dimensions of the spill tubes are: 5.9 m in height and 4.8 m in width. The spill with relevant levels and components is schematically visualized in Figure 2.5. The highest point in the spill tubes is at -3.30 m NAP, meaning the spill tubes are always submerged.

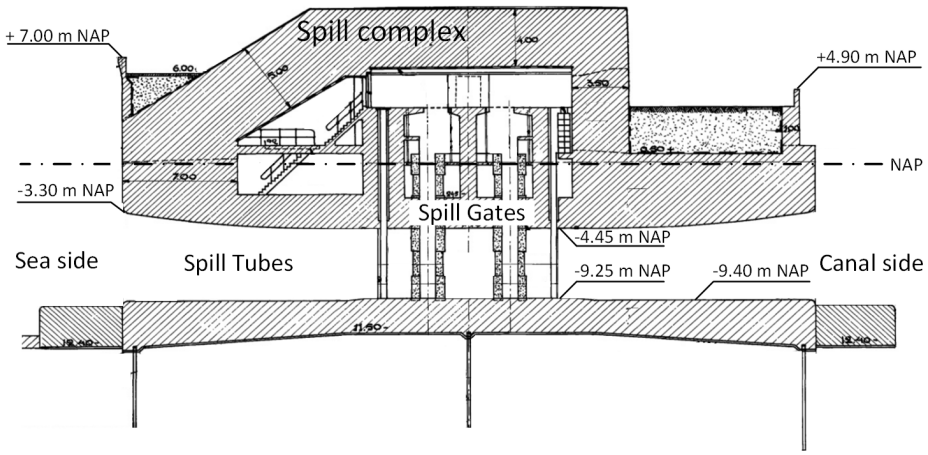

Figure 2.5: Schematical cross section of the spill complex IJmuiden (Winter, 2011)

2.4. Locking Process

The locking process of the ship locks is schematically visualized in Figure 2.6, demonstrating one locking operation from sea to the canal. In the first step the lock chamber is at sea level, after which the outer head is opened. The ship moves into the lock chamber and the outer head closes again. Than the leveling phase starts, the water is removed from the lock chamber to ensure the chamber is at the same level as the canal. After the leveling, the inner head doors open and the ship is ready to sail onto the canal. One locking cycle requires both heads to open and close once. At least one of the heads is always closed during a normal locking procedure.

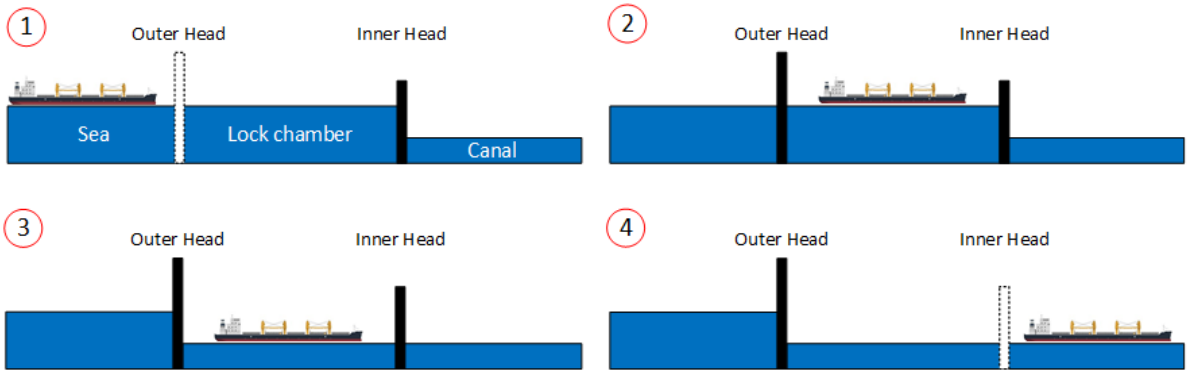

Figure 2.6: Schematic locking process

2.5. Bathymetry

The model requires a terrain representing the bathymetry, canal dimensions and side harbors. The bathymetry of the NSC and ARC are both available in a database of Rijkswaterstaat. In QGIS, the bathymetry is merged together with the topographic data from the surroundings. The topographic data is acquired from a database in the form of a height chart representing the topography of the Netherlands (AHN, 2022).

The North Sea Canal is on most sections 270 m in width and at least -15.1 m NAP in depth. Numerous side and inner harbors are located along the North Sea Canal. These side harbors contribute to the storage capability of the water system. The bathymetry of the NSC is visualized in Appendix Figure D.1, with a color gradient indicating the height differences. The Amsterdam Rhine Canal is between 100 and 120 m in width and between -5.0 m and -6.0 m NAP in depth. The bathymetry of the ARC and its surroundings is visualized in Appendix Figure D.2. The side rivers are not included in the model, as there is no bathymetry data available for the Amstel and Vecht.

3

Failure Mechanisms

This chapter outlines the different failure mechanisms for the ship locks and spill. The methods to determine the probability of failure are explained. The end of the chapter presents the storms that are used as an input for the model. The first section describes the ship lock failure, the second section describes the spill failure. As already outlined in the introduction, this research only considers two failure mechanisms: overtopping and non-closure.

For dike trajectory 44-3 (IJmuiden), the Dutch water law prescribes a lower limit flood risk of 1:10 000 (Ministry of Infrastructure and Water Management, 2025). This flood risk limit is used as a guideline for the assessment of failure of the components in the spill-lock complex. Failure of the retaining components at the spill-lock complex leads to failure of the water system in case too much sea water flows into the system.

3.1. Ship lock failure

Ship lock failure can occur due to both overtopping and non-closure. The retaining height of the fully closed ship locks is the most important parameter for failure due to overtopping. When sea water rises above the outer head (sea side) of the lock, water flows over the lock gate into the lock chamber. When a sufficient volume of water flows over the outer head into the lock chamber, the inner head on the canal side will also be subject to overtopping. The retaining height of the inner heads is lower than the outer head for all locks. However, the Nieuwe Zeesluis is an exception, as this lock has two identical gates in both heads. The retaining heights of the different heads of each lock are presented in Figure 3.1.

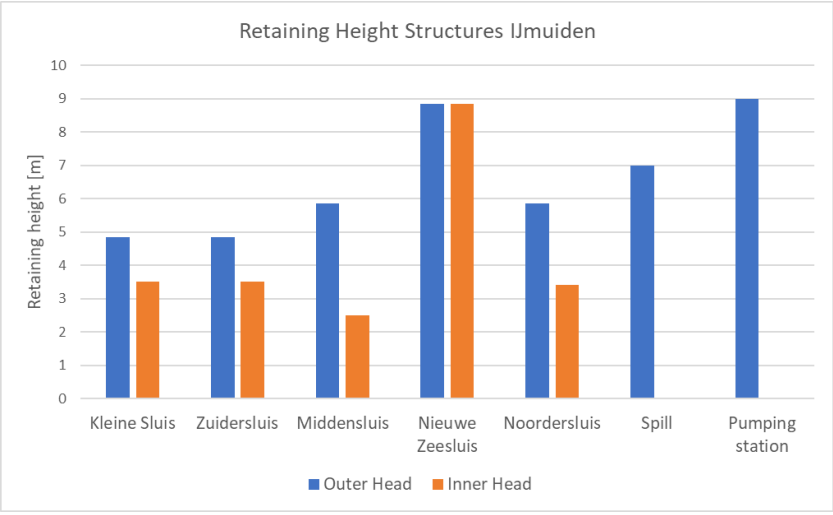

Figure 3.1: Retaining heights of components in the complex

Overtopping of the retaining structures only due to waves is not taken into account, as this volume of inflowing water is considered to have a small effect on the canal level. Failure due to overtopping is expected to start when the sea water is at least 10 cm above the retaining structure. With less overtopping, the effects on the canal water levels are marginal.

Non-closure of the outer ship lock gates causes the retaining capacity of the lock to decrease. In case the outer head is not closing, retaining must be provided by the inner head. This retaining height of the inner head is lower than the retaining height of the outer head, except for the Nieuwe Zeesluis, which is also visible in Figure 3.1. When the inner head is not closing, the full retaining capacity of the lock is still provided by the closed outer head.

3.1.1. Probabilistic Approach

The probability of failure due to overtopping or non-closure is based on the return period of the sea water level exceeding the specific retaining height. Storms with such sea water levels are not common and have a high return period. Existing research on the basic stochastics for different water systems and locations in the Netherlands presents the return periods of extreme sea water levels at IJmuiden (Chbab, 2017). The results of this research are visible in Figure 3.2, where the extreme sea water level at IJmuiden is plotted against the return period. The relevant return periods for the different retaining heights are used to determine the yearly probabilities of overtopping. The yearly probability of non-closure is built up from the probability of not closing the outer head and the yearly probability of exceeding the inner head retaining height. For both failure mechanisms the relevant failure probabilities per year are calculated.

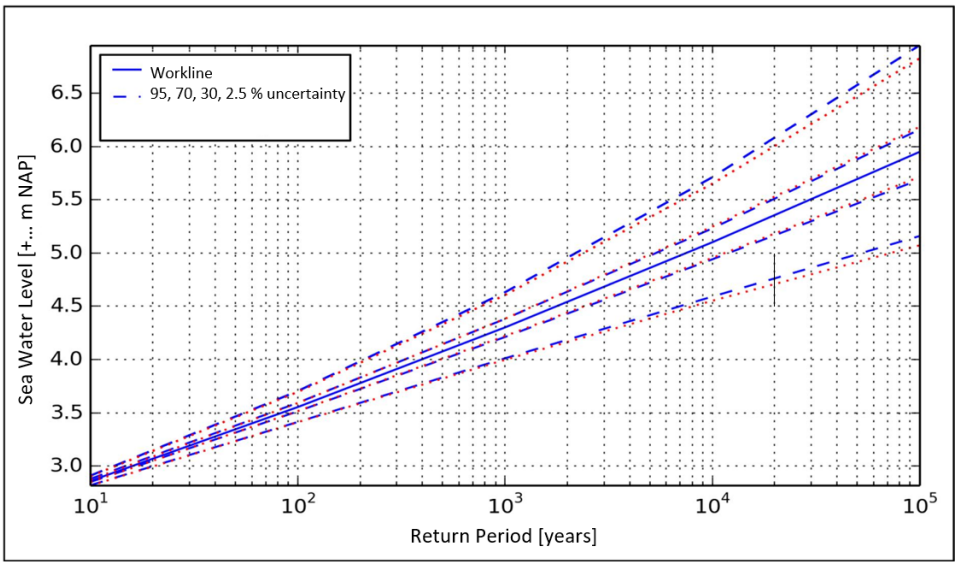

Figure 3.2: Return period of extreme sea water levels in IJmuiden (Chbab, 2017)

For overtopping the yearly probability of failure is taken equal to the yearly probability of the sea water level being 10 cm above the retaining height. This results in significant volume flowing into the system as previously discussed. In Table 3.1 the return periods and the yearly probabilities of failure for the retaining structures are presented, resulting from the extreme value analysis performed by Chbab (2017). Overtopping of the Nieuwe Zeesluis, pumping station and spill complex is not considered further, as the retaining heights are equal or higher than +7.00 m NAP. This retaining height is sufficient to withstand more than a 100 000 years returning storm. This retaining capacity is considered sufficient with respect to the guideline of 1 in 10 000 years flood risk.

Lock	Retaining Height Outer Head [m]	Return Period [years]	$P_{over,\ OH}$
Kleine Sluis	4.85	70 000	$1.4 \cdot 10^{-5}$
Zuidersluis	4.85	70 000	$1.4 \cdot 10^{-5}$
Middensluis	5.85	100 000	$1.0 \cdot 10^{-5}$
Noordersluis	5.85	100 000	$1.0 \cdot 10^{-5}$

Table 3.1: Probability of failure due to overtopping per lock

Overtopping of the rest of the outer heads comes with sea water return periods of 70 000 years and more. Compared to the guideline flood risk of 1:10 000, the focus is more on the non-closure in combination with overtopping of the inner head.

The yearly probability for non-closure consists of two components. The first component is the probability that the outer head is not closed during the storm. The yearly probability of overtopping the inner head similarly follows from the return period of extreme storm events (Chbab, 2017). The second component is similar to the yearly failure probability of overtopping, but for non-closure failure it means overtopping of the inner head. These components determine the probability of failure for non-closure, resulting in the following equation:

$$P_{f,\ NC} = P_{over,\ IH} \cdot P_{NC} \tag{3.1}$$

The probability of non-closure of the outer head is determined with the use of event trees according the method described by literature (Hill et al., 2002). The event trees per lock are presented in Appendix E. The Nieuwe Zeesluis is also not considered for non-closure, as the inner head has the same retaining height as the outer head.

The probability of non-closure is built up from the combination of the probability that the head is opened when the storm starts and that the head is not closing as requested. The probability that the outer head is initially opened is taken to be $P_{initial\ open} = 0.4$. This estimation is conservative, as the heads are expected to be closed more often during normal locking procedure.

The probability of not closing when requested is presented in the legal review of the dike system 44-3 (Van den Berg et al., 2019) and is visualized in Table 3.2, with the corresponding substantiation for every values given by the literature. These probabilities of not closing are determined by five experienced object specialists.

lock	P_{NC}	Given Substantiation
Kleine Sluis	0.001	Substantiated assumption
Zuidersluis	0.001	Substantiated assumption
Middensluis	0.003	Analysis
Noordersluis	0.002	Analysis

Table 3.2: Non-closure probabilities (Van den Berg et al., 2019)

The combination of both the $P_{over,\ IH}$ and P_{NC} is presented in Table 3.3, giving the probability of failure per year due to non-closure for the different ship locks. The return period for overtopping of the inner head of the Middensluis at +2.60 m NAP (2.50 + 0.10 m overtopping) is estimated by interpolating the data from Figure 3.2 (Chbab, 2017).

Lock	Retaining Height Inner Head [m]	Return Period [years]	$P_{over,\ IH}$	P_{NC}	$P_{f,\ NC}$
Kleine Sluis	3.5	100	$1.0 \cdot 10^{-2}$	$4.0 \cdot 10^{-4}$	$4.0 \cdot 10^{-6}$
Zuidersluis	3.5	100	$1.0 \cdot 10^{-2}$	$4.0 \cdot 10^{-4}$	$4.0 \cdot 10^{-6}$
Middensluis	2.5	1	1.0	$1.2 \cdot 10^{-3}$	$1.2 \cdot 10^{-3}$
Noordersluis	3.4	80	$1.3 \cdot 10^{-2}$	$8.0 \cdot 10^{-4}$	$1.0 \cdot 10^{-5}$

Table 3.3: Probability of failure due to non-closure per ship lock

The return period for non-closure failure of the Middensluis is approximately 833 years. Non-closure of the other locks results in return periods of 100 000 years or more. Therefore, only the failure state of non-closure of the outer head of the Middensluis is taken into account in the rest of the research when considering failure of the ship locks.

3.1.2. Storm Scenario for Non-Closure of the Outer Head of the Middensluis

The relevance of the failure scenario non-closure of the outer head of the Middensluis is checked by modeling an extreme storm event. The selected extreme storm event has a return period of 1000 years, with a maximum water level of +4.30 m NAP (Chbab, 2017). The return period of this extreme event is calculated by multiplying the return period of the non-closure of the outer head (see Table 3.3) with the return period of the storm event:

$$\frac{1}{P_{f,\ NC,\ Middensluis}} \cdot RP_{storm} = \frac{1}{1.2 \cdot 10^{-3}} \cdot 1000 = 833\ 333 \text{ years} \tag{3.2}$$

The return period of the extreme event is exceeded far beyond the guideline for flooding (10 000 years). The form of the storm surge is prescribed by research for the Eastern Scheldt Barrier located along the same North Sea coast as IJmuiden (Saman, 2017). Therefore, form of the storm surge on sea is expected to be equal for both the Eastern Scheldt location and IJmuiden. The storm surge is described by the following squared cosine function:

$$h_{sea}(t) = h_{sea,max} \cdot cos^2(\pi \cdot \frac{t}{T_{ss}}) \tag{3.3}$$

where,

h_{sea}	Sea water height	[m]
$h_{sea,max}$	Maximum sea water height	[m]
T_{ss}	Storm duration	[hours]

The storm is generated with Equation 3.3 and parameters $h_{ss,max}$ = 4.30 m and T_{ss} = 72 hours. The duration of the storm influences the volume of water flowing over the lock gate. According literature, the duration of such an extreme storm is described by a lognormal distribution with $\mu = 54.3$ and $\sigma = 18.8$ this results in: T_{ss}~LogNormal(54.3, 18.8^2) (Saman, 2017). Based on this distribution, 72 hours of storm is a considerable duration and creates an unfavorable storm to test the effect on the water system. For this extreme event model run, the tide is not considered. The results of the model run are presented in Section 4.4.1.

3.2. Spill failure

Spill failure is only relevant for failure mechanism non-closure of the spill gates. As previously discussed, overtopping of the +7.00 m NAP retaining height has a return period that convincingly exceeds the flood risk guideline. This research only considers non-closure of all seven spill gates at once, with all spill gates fully raised. Failure of less gates is not considered, but will result in a lower inflow of sea water due to less spill tubes being opened.

Non-closure of the spill gates will quickly lead to water inflow into the system. The spill gates are opened during spilling operation when the water level at the canal exceeds the water level at sea. In case non-closure of the spill gates leaves the spill tubes opened, water flows back into the water system when the sea water level exceeds the water level on the canal. The spill tubes are continuously submerged, with the spill gates opened the water always flows from the highest level towards the lowest level via the spill tubes.

3.2.1. Probabilistic Approach

The probability of failure due to non-closure of the spill gates is determined by making a comparison with the Haringvliet spills (HVS). Data about the non-closure of the HVS is available at Rijkswaterstaat. This data is generated because this structure is classified as a storm surge barrier, in contrast to the complex of IJmuiden. The probabilities of non-closure for the HVS are presented in Table 3.4. The gates are clustered together based on different types of failure. When for example the operating system experiences a shutdown, all gates are not closing via normal procedure. This scenario is incorporated into the probability that all gates are not closing. This principle also results in a higher probability that 11-17 gates are not closing compared to 3-10 gates not closing, as it is more likely that the full system fails rather than, for example, 75% of the gates. The third column of Table 3.4 presents the clustering of the spill in IJmuiden that is similar to the clustering of the Haringvliet spills. The failure probabilities for non-closure of the spill gates in IJmuiden are based on the HVS for the corresponding clusters.

Clustering HVS	$\mathbf{P_{f,\,NC,\,HVS}}$	**Clustering IJmuiden**	$\mathbf{P_{f,\,NC,\,IJmuiden}}$
1 gate not closing	$2.70 \cdot 10^{-3}$	1 gate not closing	$3 \cdot 10^{-3}$
2 gates not closing	$7.50 \cdot 10^{-4}$	2 gates not closing	$8 \cdot 10^{-4}$
3-10 gates not closing	$5.73 \cdot 10^{-6}$	3-5 gates not closing	$6 \cdot 10^{-6}$
11-17 gates not closing	$5.33 \cdot 10^{-5}$	6-7 gates not closing	$6 \cdot 10^{-5}$

Table 3.4: Non-closure probabilities HVS and IJmuiden

The failure probabilities per closure request are presented in Table 3.4. Multiplication of these probabilities with the number of closures per year results in the yearly probability of failure of the spill. Due to the existing semi-diurnal tidal cycle, the spill gates closures is limited to maximum twice a day. This closing frequency results in a maximum of 730 closures per year. However, the spill is not opened during both low tides every day. During a significant storm surge, the sea level at low tide will still exceed the canal water level. According to a database containing the closures of the spill from 1991 to 2024, the number of closures over the recent years is on average 250 closures per year. Therefore, 300 closures per year is selected to be a safe estimate, allowing for years with more closures. The amount of open spill gates prior to closure is not mentioned, therefore the assumption is made that all 300 closures are performed with all 7 spill gates together.

The yearly probability of failure due to non-closure of all 7 spill gates is: $6 \cdot 10^{-5} \cdot 300 = 1.8 \cdot 10^{-2}$ per year. The question whether the sea is high enough to cause inflow in the system at the moment of closure is not incorporated in the probability calculation. As the semi-diurnal tidal cycle results in at least two maximum sea water levels a day, which exceed the normal canal level. Additionally, the spill gates are most of the times closed, when the sea water is beginning to rise beyond the canal level. The failing of closure of the spill gates can happen unnoticed until the moment that water in the canal starts rising, at which point the failure is identified. This also occurred during the failure of 2 November 2023.

3.2.2. Storm Scenarios for Non-closure of the Spill

Compared to the storm scenario selection for non-closure of the Middensluis, there is a different approach in selecting the storm scenarios for non-closure failure of the spill. As previously discussed, high water in combination with opened spill gates causes inflow of sea water into the system, due to the submerged position of the spill tubes. Because of this relation, non-closure of the spill gates is not linked to extreme storm events.

At the beginning of a storm there has to be a spilling window. If the storm surge causes the sea level

at the beginning of the storm to exceed the canal level, the spill remains in closed position. Spilling is only performed when the difference between the canal and sea is equal or bigger than 16 cm. Using the target level of the canal, it means that the sea level is at least -0.56 m NAP at the beginning of the storm.

The storm setup is generated by using the same form as used for the storm surge in Equation 3.3 (Saman, 2017):

$$h_{setup}(t) = h_{setup,max} \cdot cos^2(\pi \cdot \frac{t}{T_{storm}}) \tag{3.4}$$

The storms are generated by adding a standard tidal cycle to the different storm surges. The tide and storm surge are combined with the use of a phase difference φ, indicating the difference between the maximum of the surge and the maximum of the tide in hours ($\varphi = t_{max,\ surge} - t_{tide}$). The phase difference has a standard distribution as presented in Table 3.5 (Bakker et al., 2025).

φ	-6	-5	-4	-3	-2	-1	0	1	2	3	4	5	6
P	0.007	0.027	0.055	0.096	0.103	0.171	0.034	0.041	0.034	0.055	0.123	0.164	0.089

Table 3.5: Discrete distribution of the phase difference (Bakker et al., 2025)

The storms are generated by varying the parameters of Equation 3.4. The duration of the storms is taken as a constant at 30 hours. This duration allows the storm to reach its maximum relatively fast, providing a significant inflow through the spill tubes, despite short duration openings. The $h_{setup,max}$ is varied between 0.0 and 2.0 m with a step size of 0.5 m. The tide is varied between three states: neap, intermediate and spring tide. All parameters and their variations for the storm generation are summarized in Table 3.6.

Parameter	Unit	Range
$h_{setup,max}$	meter	[0, 0.5, 1.0, 1.5, 2.0]
φ	hour	[-6, -5, -4, ..., 4, 5, 6]
T_{storm}	hour	30
Tide	-	[neap, intermediate, spring]

Table 3.6: Parameters storm generation spill

With the combination of all parameters, 159 storms are generated. These storms are filtered on the presence of a spill window at the beginning of the storms as already discussed earlier. The spill window is present when the sea water level drops below -0.56 m NAP at the start of the storm. After the selection on the presence of a spilling window, 38 storms remain.

To see the first effect of different failure durations on the water levels on the canal, eight storms were selected based on a varying range of $h_{max,\ storm}$ values. These storms are presented in Table 3.7. h_{max} is the height of the first peak directly after the spill window, meaning that h_{max} is not the maximum of the whole storm, but the maximum peak during failure.

The probability of occurrence of each individual storm is calculated by using the relevant probabilities for every parameter. The multiplication of P_{setup}, P_{φ} and P_{tide} gives the probability per storm. P_{setup} follows from the analysis of 20 years of data, where the calculated astronomical sequence is subtracted from the measured sea water level to obtain the water levels only due to the influence of the setup. P_{φ} is distributed according Table 3.5. P_{tide} is a constant for the three standard tides chosen. $P_{tide,\ spring}$ and $P_{tide,\ neap}$ have a probability of occurrence of 0.25. $P_{tide,\ intermediate}$ represents the intermediate tides, $P_{tide,\ intermediate}$ = 0.50. The calculated probabilities for the selected storm scenarios are presented in Table 3.7.

Scenario	h_{setup} [... m NAP]	φ	Tide	h_{max} [... m NAP]	$P_{occurrence}$
1	0.50	-4	intermediate	1.18	0.00738
2	0.50	-6	intermediate	1.28	0.00094
3	1.00	-5	intermediate	1.48	0.00242
4	1.00	-6	intermediate	1.59	0.00063
5	1.50	-5	intermediate	1.73	0.00137
6	1.00	6	spring	1.86	0.00399
7	2.00	-5	intermediate	1.99	0.00071
8	2.00	-6	intermediate	2.20	0.00013

Table 3.7: Storm scenarios non-closure spill

The failure duration is the amount of time that the spill gates are opened while water is flowing in, until the moment that the gates are closed. In this research three different failure durations are compared, 3, 6 and 12 hours of failure. The results of the model for the storm scenarios and the different failure durations are presented in Chapter 4.

4

Model

This chapter presents the configuration, calibration and validation of the model used to simulate the water levels in the NSC and ARC during failure of the spill-lock complex. There are a few requirements for the model to ensure reliable and relevant simulations. First of all, the model should perform 2D unsteady flow calculations. Additionally, the model is required to run multiple scenarios at a respectable computational time. The model is also expected to return water levels along different locations in the water system. Finally, the model must demonstrate the behavior of the flood wave through the water system. Water levels at sea provide the input, while the model computes, among others, the inflowing discharge through the spill and over the lock gates.

An suitable free-to-use modeling software that contains all discussed requirements is the HEC-RAS software. The model is developed with software version: HEC-RAS 6.6. The HEC-RAS software is specialized in numerical computation of hydraulics of rivers and canals. In the model it is possible to add structures similar to the spill and ship lock gates located in IJmuiden. HEC-RAS performs 2D unsteady flow analysis and returns a simulation of the behavior of the flood wave.

4.1. Model Configuration

The terrain of the model is based on the bathymetry data of the North Sea Canal and Amsterdam Rhine Canal with the adjacent harbors and small storage areas as visualized in Appendix D. The model extends from the outer harbor of IJmuiden to the Irene locks, located close to Wijk bij Duurstede. A mesh grid is applied across the canal and harbors to perform the numerical 2D analysis. The mesh is automatically generated with a cell size of 20 by 20 meters. The cell size is 1/5 of the width of the ARC and approximately 1/14 of the width of the NSC. Due to the large area of the water system, the mesh is considered sufficiently detailed, while keeping the computation time acceptable. The grid size is reduced near the structures at the spill-lock complex IJmuiden to model the variable flow over the lock and behind the spill tubes in greater detail.

At the location of the spill-lock complex, the structures are generated in the model with similar dimensions and positioning. Furthermore, a boundary condition is added, describing the durations of opened spill gates during failure. The lock gate is modeled in the form of a narrow weir, with similar dimensions as the Middensluis. When sea water exceeds the retaining height of the lock gate, it flows over the modeled weir, into the water system. A pump is also added to simulate the behavior of the system after failure when the system tries to restore its normal water levels.

The locations where water levels are requested from the model correspond to the measurements station locations, which are used by Rijkswaterstaat for data collection. These locations are presented in Figure 4.1. The used measurement stations in the canal are: IJmuiden Buitenhaven, Buitenhuizen, Amsterdam Surinamekade, Weesp and Maarssen. The data of the measurements stations is used to calibrate the model (Rijkswaterstaat, 2024), therefore the same locations are used as output locations for the model. The locations are spread across the water system, allowing for a good presentation of the behavior of the flood wave through the entire system.

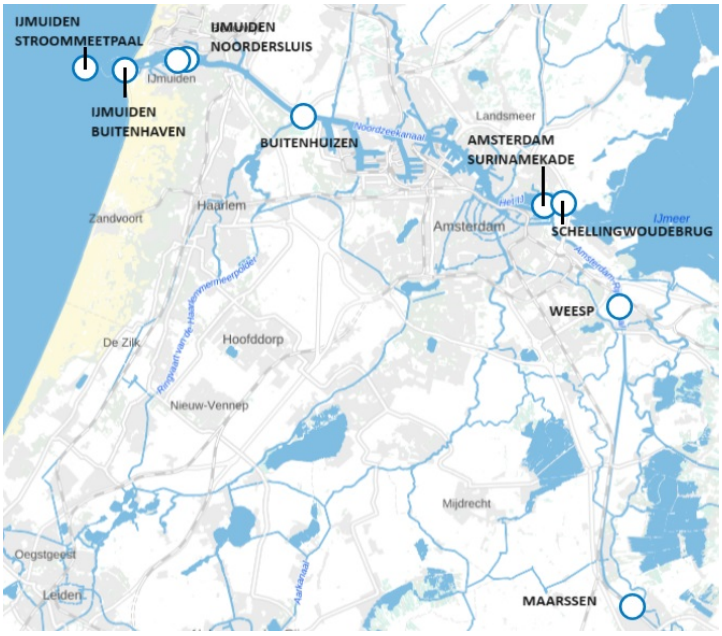

Figure 4.1: Measurement stations along the canal (Rijkswaterstaat, 2024)

4.2. Model Calibration

The model is calibrated with the measurements from the 2nd of November 2023. These measurements provide a rare insight in the response of the system to a failure event, where the spill gates are opened in combination with the sea level exceeding -0.40 m NAP for a considerable amount of time. The output of the model is visually compared to the actual measured water levels in the canal. After the first configuration, the model did not result in similar water levels. This deviation was caused by two essential computation settings in the model, the computation interval and the used equation set. The process of calibration of the model is described in the following subsections.

The model contains several (boundary) conditions. The first boundary condition is the water level at sea during failure, which is obtained from the measurements of the sea level at the 2nd of November 2023 (Rijkswaterstaat, 2024). Another condition represents the duration of opened spill gates. The spill gates are opened and closed similar to the failure event on the 2nd of November 2023, closure occurred at 07:20 in the morning. The pump in the system is activated at the moment that the spill gates are closed, modeling the system, restoring its target water level. In the first iterations, pumping was performed at maximum capacity after closure of the structures. The initial water level in the system is -0.40 m NAP, in accordance with the conditions during the real event.

4.2.1. Computational Time Interval

The selection of the computation interval is important, as the model needs to balance between high precision and acceptable computation times. A lower computation interval increases the amount of detail in the final result, however leads to longer total computation times. In this model, the standard computation interval is set to 10 seconds. The interval can be varied and controlled with the use of the Courant number, while the modeling is ongoing. With this process, the most favorable interval is selected during computation to create a more efficient model. The Courant number is calculated according Equation 4.1:

$$C = \frac{v_w \cdot \Delta t}{\Delta x} \tag{4.1}$$

where,

C	Courant number	$[-]$
v_w	Wave velocity	$[m/s]$
Δt	Time step	$[s]$
Δx	Distance step	$[m]$

The Courant number is evaluated with every computation step. The Courant number compares the distance traveled by the wave in a single time step with the size of one grid cell. If the Courant number is smaller than 1, the wave speed is sufficiently low to ensure that the modeled information is not skipping any grid cell within a single computation step, thereby securing stability of the computation. When the Courant number reduces close to 0, the model chooses to increase the computation time step, making sure to maintain: $C \leq 1$. Increasing the computation time step reduces the total computation time of the model. If $C \geq 1$, the wave is able to skip at least one grid cell, and the computation time step needs to be reduced to maintain stable calculations. With the use of the Courant number, the model continuously assesses whether adjustment of the computation time step is feasible and required.

4.2.2. Equation Set

The available set of equations in HEC-RAS includes the Diffusion Wave Equations (DWE) and the Shallow Water Equations (SWE). The Diffusion Wave Equations are selected by default in HEC-RAS. The DWE assume that acceleration and inertial terms can be neglected, resulting in more simple water equations. The DWE in terms of the discharge is presented as Equation 4.2.

$$\frac{\partial Q}{\partial t} + U\frac{\partial Q}{\partial x} = D_t\frac{\partial^2 Q}{\partial x^2} \tag{4.2}$$

where,

Q	Discharge	$[m^3/s]$
U	Velocity of the diffusion wave	$[m/s]$
D_t	Diffusion Coefficient	$[m^2/s]$

The advantage of the DWE set is that it yields faster and more stable calculations. The disadvantage is that it is only applicable for simplified and low dynamical flow. In Figure 4.2, the modeled diffusion wave is compared with the measurements of 2 November 2023. The modeled water level follows a similar shape as the measured data. However, the detail necessary to model events such as internal reflecting waves is not available with the use of the DWE set. Therefore, the SWE set should be used to model with increased detail to better represent the measured data.

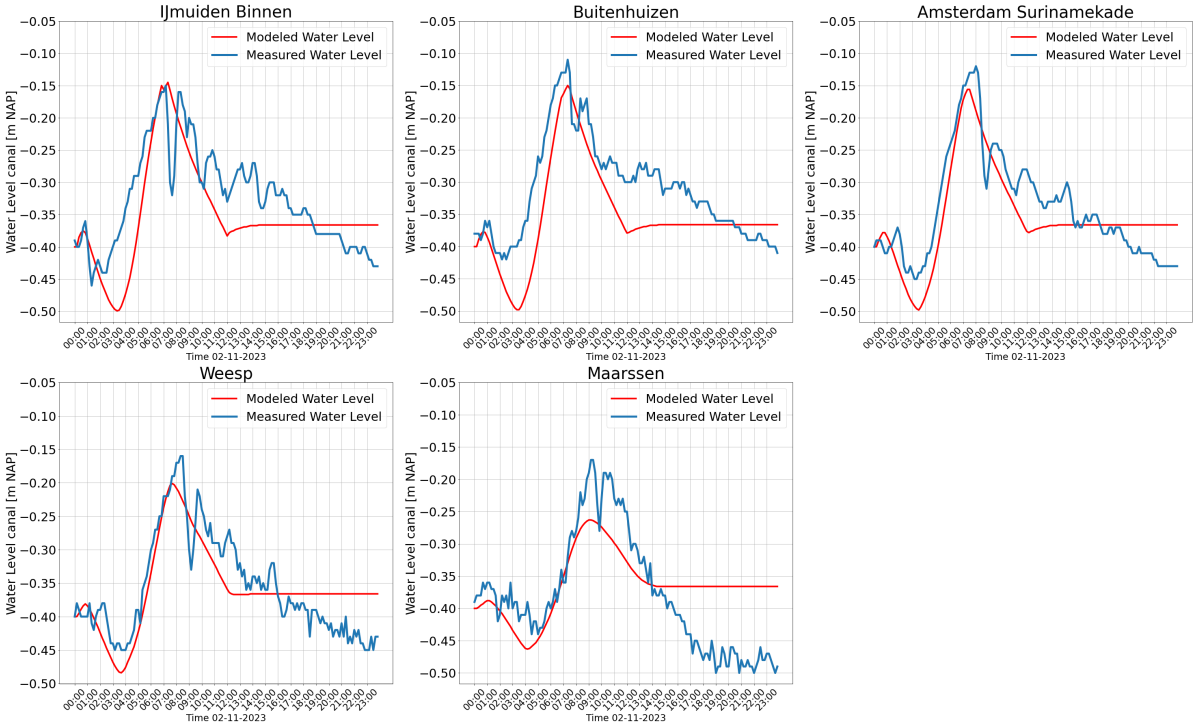

Figure 4.2: Diffusion wave comparison

The Shallow Water Equations are available in HEC-RAS in three versions. The first version is the Eulerian-Lagrangian approach, the second uses the Eulerian method, and the third version incorporates a local inertia approximation. The Eulerian-Lagrangian approach is the original and faster method. The Eulerian approach uses a more stricter momentum equation. The third version simplifies the momentum equation by neglecting the advection, diffusion and Coriolis term. The Eulerian-Lagrangian approach is the most efficient option, while the results for the compared approaches where similar. Figure 4.3 presents the model using the Shallow Water Equations with the Eulerian-Lagrangian method. This SWE simulation clearly indicates more similarities with the measured data, compared to the use of the DWE. Also the pumping station is configured to pump longer to better represent the system restoring towards its target level.

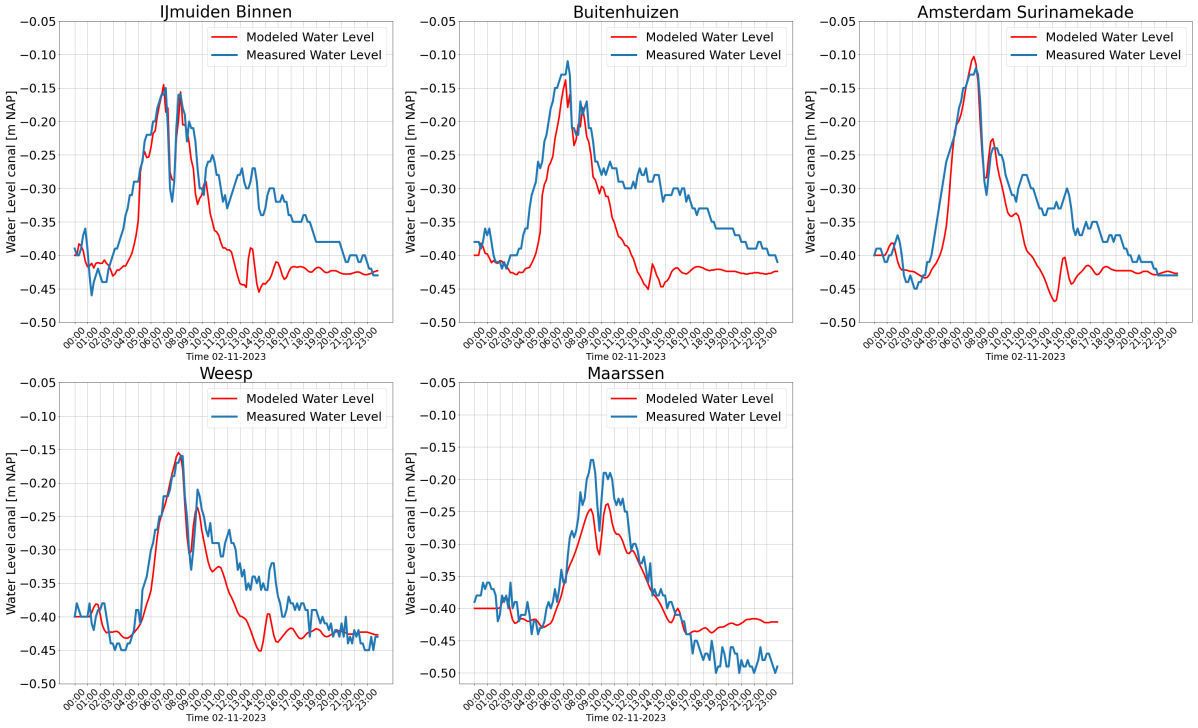

Figure 4.3: SWE ELM wave comparison

4.2.3. Pump Behavior

The final aspect of calibration lies in the tail of the water level curves. At the moment of closure, the water level in the system needs to decrease, in the model the pumps are used for modeling this process. In reality, there are multiple possibilities to reduce the water level of the system, however for simplicity, this model only takes into account the use of the pumps at IJmuiden. In Figure 4.3, pumping is performed at a constant maximum capacity of 260 m^3/s from the moment that the gates where closed (from 07:20) until the water level was restored at the target level. This pump performance clearly overestimates the rate of water removed from the system and needs to be adjusted. The overestimation is deemed to be a result of the assumption that the pumps are pumping constantly at maximum capacity, which is in practice not feasible. Furthermore, additional inflow in the water system (i.e. from the polders) is not taken into account in the model, increasing the total volume to be pumped out of the system. These assumptions result in a difference between the simulation and reality. The pumping rate is reduced to calibrate the model in the tail. The best calibration was acquired with the use of a constant pumping rate of 150 m^3/s. This calibration is visualized in Figure 4.4 and with this last step the model is deemed sufficiently calibrated for the purpose of this research.

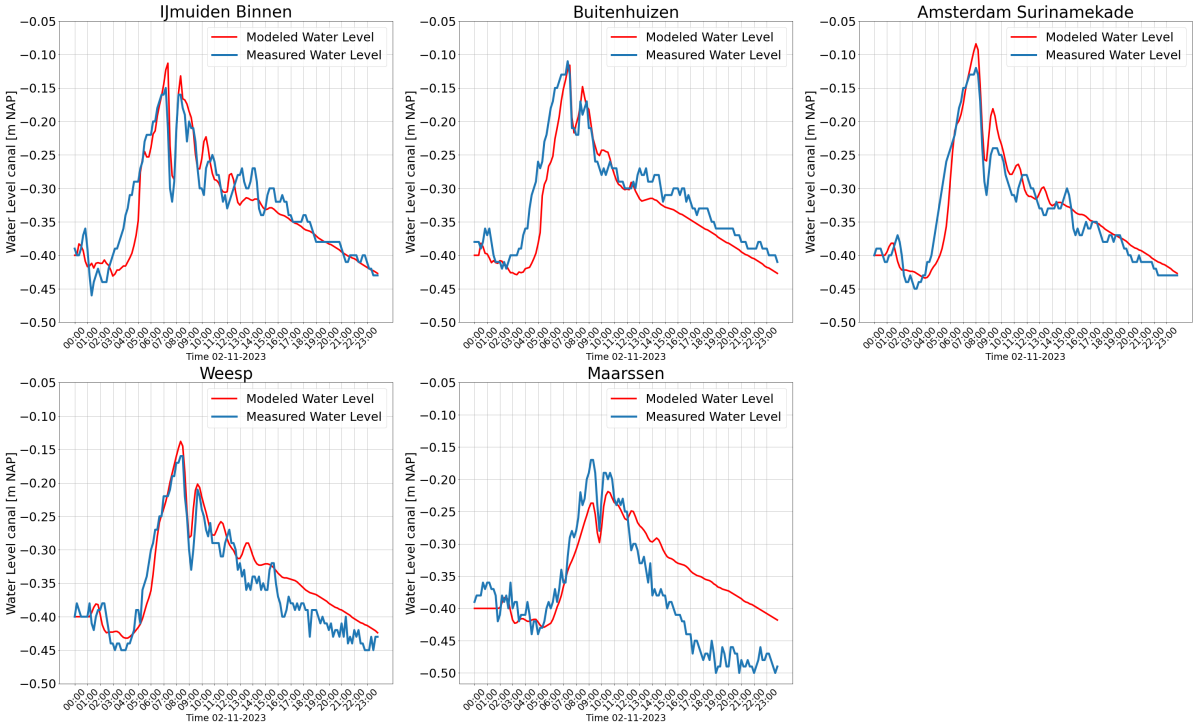

Figure 4.4: SWE Pump behavior calibration

The largest deviation between the model and the measured data is noticeable for the location Maarssen, particular in the tail of the water levels. Maarssen is located at the greatest distance from the spill-lock complex at IJmuiden, therefore little deviations between the model and reality along the system will be exaggerated. Also not including the Vecht (and Amstel) in the model calculations leads to deviations between the model and reality for the locations along the Amsterdam Rhine Canal.

4.3. Model Validation

Additional data to validate the reliability of the model results is not available. Based on the storm event, it is evident that the further the location is positioned away from IJmuiden, the larger the deviation between the model and reality occurs. Nonetheless, the peak water levels and an estimation of the duration of high water are most important in determining the effects for this research.

4.4. Model Simulations

This section presents the results of the model simulations for the selected storm scenarios presented in Sections 3.1.2 and 3.2.2. For the spill simulations, the duration of the spill gates opening is varied between 3, 6 and 12 hours. The start of opening is determined to be equal to the start of sea water exceeding the canal level. This moment is selected, as failure is most of the time recognized after the canal water level is rising unexpected. The duration of the failure depends among others on the moment of failure, the cause of failure and the time required to restore the closed position of the spill gates. For example, whether the failure happens during daytime or nighttime affect the response. The availability of water managers and mechanics on site is critical, as these people play a key role in noticing, locating and resolving the failure.

4.4.1. Model Runs Non-Closure Middensluis

Modeling the extreme failure scenario presented in Section 3.1.2 addresses the relevance to consider failure of the Middensluis in subsequent analysis. The result of the simulation is visualized in Figure 4.5. The result is only presented for the location: Amsterdam Surinamekade.

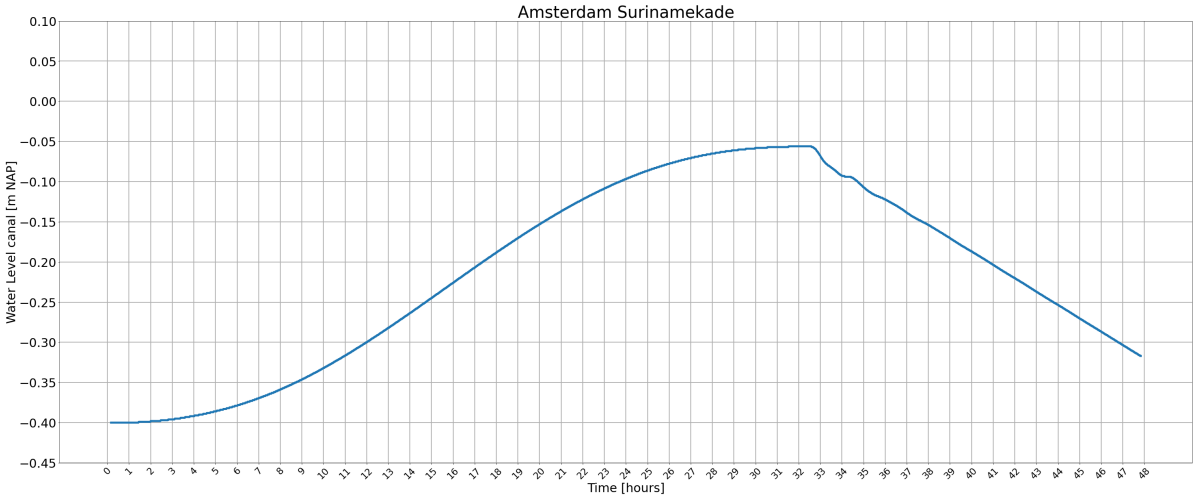

Figure 4.5: Water level on the canal due to the extreme storm scenario (H=4.3m, T=72h) and non-closure of the Middensluis

The pumping station at IJmuiden is only active when the extreme storm is damping out. The pump only operates to a certain head difference between the sea and canal. This difference is to high during the peak of the storm.

In the model, the initial water level at the canal is set to: -0.40 m NAP. When a large storm is forecast, the decision can be made to pump out water from the canal in advance to the minimum level of: -0.55 m NAP (see Table 2.1). This strategic measure creates more buffer for the canal and provides a simple solution to reduce the possible impact of failure of a similar extreme storm event. The highest water level on the canal is -0.06 m NAP for a short duration of time. When the canal was lowered to -0.55 m NAP before the storm event, the maximum water level on the canal could be reduced up to approximately -0.20 m NAP.

Considering the possible reduction of the canal level and the high return period for such an extreme event, the effects of non-closure of the ship locks are considered to be acceptable. Therefore, failure due to Non-Closure of the Middensluis is not further considered in this research.

4.4.2. Model Runs Non-Closure Spill

The scenarios from Section 3.2.2 are used as input for the model and result in the modeled water levels for the different locations along the canal. The water levels of the water system for 3 hours of spill failure are presented in the graphs in Figure 4.6. The same graphs are enlarged in Appendix F. The locations of the water level outputs are selected as previously discussed in section 4.1. The locations are abbreviated in the tables as follows: IJmuiden Binnen (IJBNN), Buitenhuizen (BTHZN), Amsterdam Surinamekade (SRNMKD), Weesp (WSP) and Maarssen (MRSN).

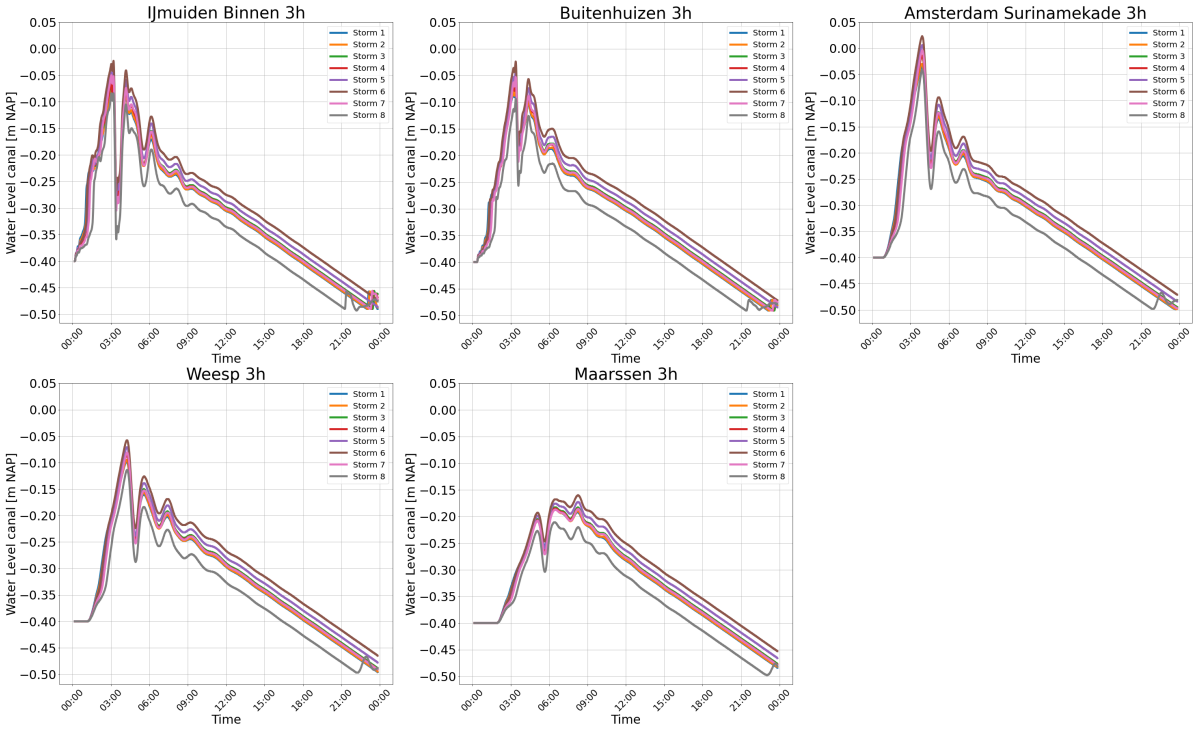

Figure 4.6: Water levels throughout the water system for 3 hours of spill failure

Scenario	$h_{max,canal}$ [... m NAP]					Mean Duration High Water [h]
	IJBNN	**BTHZN**	**SRNMKD**	**WSP**	**MRSN**	
1	-0.082	-0.077	-0.036	-0.098	-0.186	18
2	-0.078	-0.071	-0.030	-0.095	-0.185	18
3	-0.063	-0.059	-0.015	-0.085	-0.183	18
4	-0.065	-0.060	-0.014	-0.086	-0.185	18
5	-0.040	-0.041	0.006	-0.071	-0.173	19
6	-0.023	-0.024	0.023	-0.058	-0.160	20
7	-0.050	-0.053	-0.004	-0.081	-0.186	18
8	-0.084	-0.094	-0.042	-0.114	-0.211	16

Table 4.1: Model simulations for 3 hours of spill failure

The modeled water levels for 3 hours of spill failure demonstrate similar distributions. The maxima of all storms on the NSC is in the range of -0.10 and 0.00 m NAP. On the ARC the maxima range between -0.15 and -0.05 m NAP. Given that the failure only lasts 3 hours, the sea water is still rising at the moment of gate closure, therefore the storm maximum is not yet reached.

For these short durations of failure, the impact of the storms is mainly related to the early stage, where the water levels are rising towards their maximum. The storm rise is largely dependent on the duration of the storm, for instance, a short storm duration results in the storms reaching their maximum earlier. However, for spill failure the storm duration is taken as a constant: 30 hours. This constant storm duration explains the similar water level distributions for the 3 hour spill failure. The results for 6 hours of spill failure are presented in Figure 4.7.

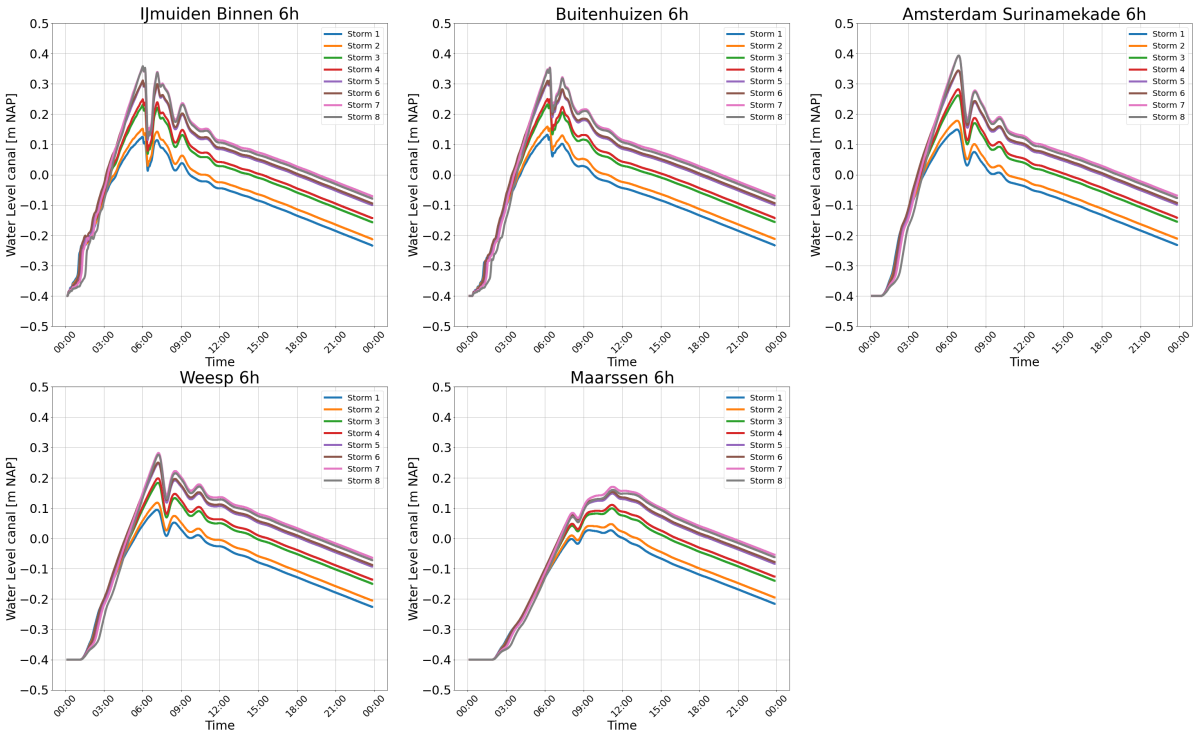

Figure 4.7: Water levels throughout the water system for 6 hours of spill failure

Scenario	$h_{max,canal}$ [... m NAP]					Mean Duration High Water [h]
	IJBNN	**BTHZN**	**SRNMKD**	**WSP**	**MRSN**	
1	0.125	0.132	0.149	0.094	0.027	35
2	0.152	0.159	0.178	0.118	0.047	36
3	0.231	0.232	0.262	0.183	0.099	39
4	0.249	0.250	0.282	0.198	0.111	39
5	0.309	0.308	0.343	0.247	0.148	42
6	0.311	0.311	0.344	0.250	0.160	42
7	0.357	0.354	0.393	0.282	0.170	44
8	0.358	0.352	0.393	0.276	0.160	44

Table 4.2: Model simulations for 6 hours of spill failure

For 6 hours of spill failure, the effect due to the different storm maxima is more clear. The water level distributions start similar, while after some time the maximum level of the storms determines the maximum of the water level on the water system. The maximum water levels on the NSC are in the range between +0.10 and +0.35 m NAP, the levels on the ARC are between +0.10 and +0.30 m NAP. The results for 12 hours of spill failure are presented in Figure 4.8.

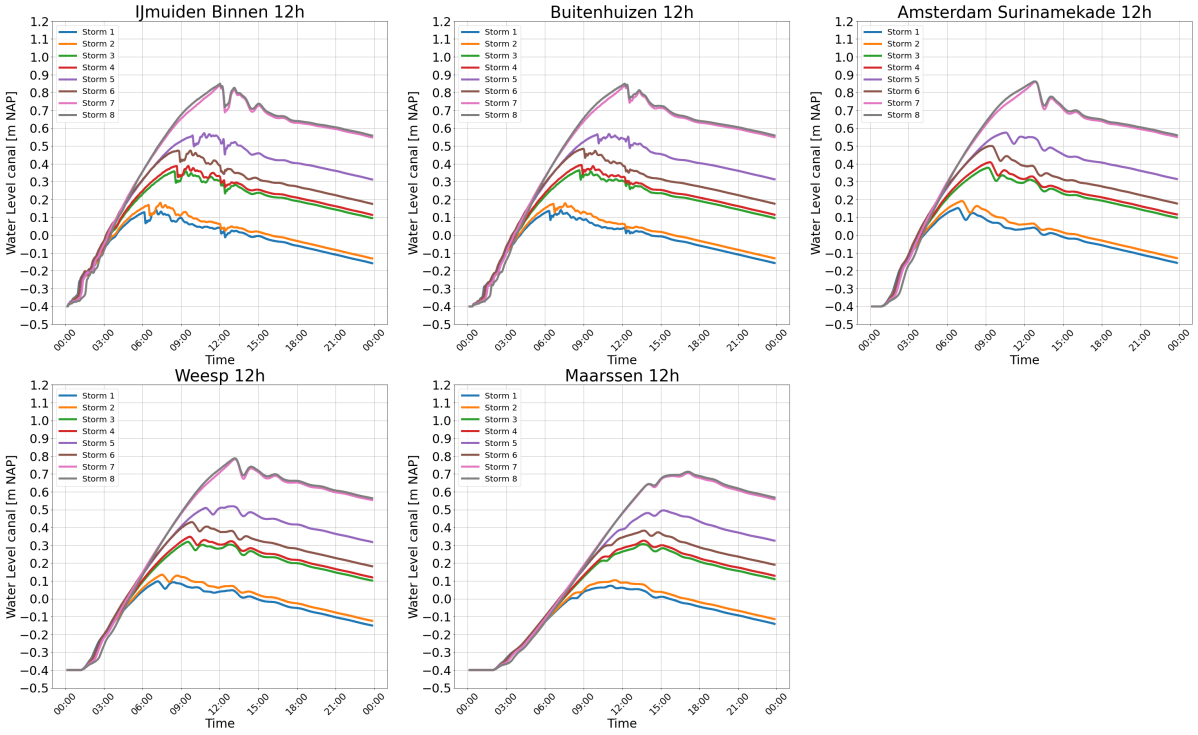

Figure 4.8: Water levels throughout the water system for 12 hours of spill failure

Scenario	$h_{max,canal}$ [... m NAP]					Mean Duration High Water [h]
	IJBNN	**BTHZN**	**SRNMKD**	**WSP**	**MRSN**	
1	0.143	0.140	0.152	0.098	0.073	39
2	0.181	0.179	0.191	0.135	0.104	40
3	0.358	0.364	0.378	0.320	0.307	54
4	0.388	0.394	0.409	0.348	0.326	55
5	0.572	0.567	0.575	0.519	0.496	67
6	0.474	0.484	0.500	0.430	0.382	58
7	0.842	0.838	0.859	0.783	0.705	81
8	0.850	0.849	0.862	0.788	0.713	81

Table 4.3: Model simulations for 12 hours of spill failure

For 12 hours of failure the results demonstrate a similar behavior as the results for 6 hours of failure, however the reached water levels in the water system are higher. Additionally, the tidal behavior is more dominant for the lower storm surges, compared to the high surges. Low tide during the smaller storm surges results in lower sea levels compared to the canal. During this low tide period, water is able to flow back into the sea. The maxima at the NSC lie between +0.10 m NAP and +0.85 m NAP and at the ARC the maxima lie in between +0.10 and +0.80 m NAP. The maxima +0.85 and +0.80 m NAP are extreme levels at the canal and will cause (local) flooding in the water system. The impact of the flooding on the water levels in the system is not included in the model.

4.4.3. Flood Wave Behavior

For the three different failure durations, there is a similar start of the water level rise at the canal. The first hours of failure depend on the shape of the storm. Due to the constant storm duration, the start of the storm distributions is similar for all storms. For the 3 and 6 hours failure duration, the maximum level at the canal is reached at the closing of the spill gates. For the lower storms in combination with the 12 hours of failure, the maximum canal level is already reached before closure. During these 12 hours of failure, the storm peak on the sea can already drop below the canal level, allowing for spilling during opened gates.

The water level distributions have a steep inclination at the beginning of failure. The water level of +0.00 m NAP on the NSC is already reached after 3 to 4 hours, within 5 to 8 hours the same water level is reached on the ARC. The flood wave travels gradually through the system, which can be seen when comparing the time of the maxima at the different locations. Within a few hours, the wave is able to reach through the whole system.

A smaller wave is generated by the sudden closure of the spill gates. After closure a sudden drop in water level is visible for IJmuiden Binnen, this drop forms a wave that travels upstream through the canal. Due to reflection in the closed system, this wave is able to travel back and forth through the system. As the generated wave travels, the movement dies out over time.

After the analysis of the 8 storms, a few remarks can be made. The failure scenarios result in significant water level rise on the water system. With 3 hours of failure duration, the water level rise is dominated by the shape of the storm. However, this research does not vary the duration of the storm, which has an influence on the shape of the storm. Regarding the 12 hour duration of failure, it is expected that failure will not take as long as 12 hours due to the incident at the 2nd of November 2023. The incident has been a wake-up call for the operators and responsible crisis managers. In case a failure scenario regarding the non-closure of the spill gates occurs again, it is expected that the duration of failure will be somewhere between 3 and 6 hours. Next to that, it is unlikely that all spill gates will remain opened for 12 hours, as the gates can always be lowered manually with the use of gravity. The scenario of 12 hours of failure of all spill gates is highly unlikely. For these discussed reasons, the 6 hour failure duration of the spill is selected to work out in further detail.

5

Effects

This chapter outlines the effects of failure resulting from the failure mechanisms as discussed in Chapter 3. The modeled water levels due to 6 hours of spill failure are linked to the effects of such failure. This chapter formulates an answer to the third sub-question and is required to determine the flood risk of the water system. Damage due to flooding is difficult to estimate and poses threats to different factors. The primary sources of damage are discussed in this chapter, together with the estimation for the costs of damage.

5.1. Water System

The model determines the water levels on the NSC and ARC due to failure, nonetheless the water system consists of more than only the two main canals. The side rivers, the Amstel and Vecht also contribute significantly to the water system. With the use of the Dutch national height database (AHN, 2022), retaining levees along the system are studied to identify the critical flooding locations. Besides direct flooding of the canal levees, there are other sources of damage that cause nuisance along the system. The damages for every component of the water system are highlighted in this section.

5.1.1. Main Canals

Apart from the critical flood locations, the levees and quays along the NSC are at minimum +0.90 m NAP. These critical flood locations are discussed in the following section. The levees and quays of the NSC are sufficiently high to withstand the maximum water levels of +0.35 m NAP during 6 hours of failure. Nonetheless, a residential area is located along the NSC, which is in direct connection with the canal. This area is called the *Houthavens*, where the houses are designed to withstand a water level of +0.80 m NAP (Kok et al., 2021). For the modeled failure scenarios, the area is expected to only experience some nuisance of water standing against the houses.

Apart from the critical flood locations, the minimal retaining height of the levees and quays along the Amsterdam Rhine Canal is +0.70 m NAP. For the modeled failure scenarios of 6 hours, the maximum water level of +0.30 m NAP will not cause flooding of the levees or quays. The lower retaining sections are located next to agricultural land. Residential areas and cities along the canal are protected by higher levees and quays. As residential areas result in higher damages, these locations are better protected against flooding. A difference between the NSC and the ARC is the presence of bridges spanning the ARC, where the NSC only has tunnels and inland ferries to connect the two banks. One of the lowest bridges over the ARC is the viaduct *Muiden* at a height of +8.65 m NAP. The required vertical clearance under the bridges for the V, VI and VII-type vessels is 9.10 m (Koedijk, 2020). With the ARC at -0.40 m NAP, the viaduct *Muiden* provides a vertical clearance of 9.05 m. When the water at the canal rises to +0.30 m NAP, the clearance reduces to 8.35 m. Therefore, the higher water levels on the canal will obstruct the biggest ships to sail underneath certain bridges.

5.1.2. Main Side Rivers

There is a critical difference between the two main side rivers. With the closing of the so-called *IJfront* and *ARC front*, the Amstel and its tributaries are disconnected from the NSC and ARC. This disconnection is established in case of high water levels at the canal of -0.20 m NAP and higher (Van Beekvelt et al., 2022). The whole Amstel basin is able to pump excess water out towards the Markermeer via pumping station Zeeburg, while still maintaining disconnected from the NSC and ARC. Due to the ability to separately pump the water out of the Amstel basin, excess water from the polders connected to the Amstel is still discharged out. With the *IJfront* closed, the center of Amsterdam is also disconnected from the NSC. The *IJfront* is visualized in Figure 5.1. Due to the closure of the *IJfront* and *ARC front* damage due to flooding in these areas is expected to be limited.

Figure 5.1: *IJfront* Amsterdam (Waternet)

The Vecht is in continuous open connection with the ARC (Neelen & Schuurmans, 2006), however, the Vecht is not represented in the model. Therefore, the water levels at the Vecht are assumed to correspond to the water levels at the ARC. This assumption might overestimate the water levels on the Vecht, as the connection between the ARC and Vecht are narrow and may not sufficiently facilitate the equal spreading of the water across the increased flow area. Additionally, if the Vecht would be included in the model, the total storage capacity would increase, which would result in lower water levels on the ARC.

The maximum water level at the ARC due to 6 hours of spill failure is approximately +0.30 m NAP. On the Vecht, several critical locations and houses may experience nuisance due to the increased water levels at the Vecht. First of all, the lowest retaining levee found along the Vecht is approximately +0.35 m NAP. The lower levees are located near agricultural land, which limits the damage in case some local flooding might occur. Due to local variations, these levees might be overtopped, but by a limited volume of water. Additionally, numerous houseboats are located along the Vecht. When the water rises quickly, the anchorage designed for lower water levels can pose a problem. Also many houses are located directly to the Vecht, where the garden is in between the river and the houses. Most houses are built somewhat higher than the gardens.

When the water suddenly rises to unconventional heights, the retaining capability of the regional water retainers in the water system are tested. For example, the retaining structures forming the *IJfront* and *ARC front* must maintain disconnection during a closure event of the fronts. Similarly, the retaining levees along the Vecht are also tested to the limit. Failure of any of these regional retaining structure results in flooding of the protected hinterland, leading to increased damages and costs.

5.1.3. Polders

When the water levels in the canal are expected to exceed +0.00 m NAP, a pumping stop of the pumping stations from the polders is ordered by Rijkswaterstaat (Van Beekvelt et al., 2022). This pumping stop disconnects the polders from the main water system that provides their drainage. Excess water needs to be stored temporary in the polders, until the moment that the pumping stop is withdrawn. The water that is required to be stored is largely dependent on the precipitation during the pumping stop. The capacity for each polder relates to the size of the polder, the water level at the start of the pumping stop and the potential damage in the area. Research is performed in the program Smart Water Management (Dutch: Slim Water Management) from Rijkswaterstaat by Hydrologic BV. (2021) on the use of certain low impact polders to store the total excess water to minimize damage in the more critical polders. This research also presents the damage per polder as a result of a certain volume to store. The research on the effects of damages in the polders as a result of the pumping stop and precipitation is outside the scope of this research. Due to the low durations of high water at the canal, the pumping stop is only active for a limited duration of time, therefore, the effects are expected to be acceptable.

5.1.4. Additional Damages

Salinization of the fresh water in the water system poses a threat to multiple facilities along the system. Normally, fresh canal water is extracted through intakes for agricultural purposes. Drinking water treatment plants (DWTPs) also use the fresh surface water to process into drinking water (Kok et al., 2021). Within the water system, such a DWTP is located along the ARC. Most of the drinking water facilities are not designed to filter salt or brackish water. Furthermore, nature experience problems with saline water in the system, most plant and animal species are dependent on fresh water for survival. The intrusion of saline water due to spill failure has to be studied in further detail.

An additional problem that arises with elevated water levels is the flooding of sewage systems that are connected (indirectly) to the canal. When water in the canal rises above a certain level, the sewage system can experience flooding, causing water inflow in the buildings and subsequent damages. The internal canals in Amsterdam are protected from flowing over, due to the 'IJfront' closure at -0.20 m NAP on the NSC (Kok et al., 2021).

5.2. Critical Flood Locations

In the previous sections the main flood protection levees were covered. Nonetheless, there are some critical locations in the water system where flooding will happen first. A qualitative analysis helps identifying the damages in case of extreme high waters in the system. The increased water levels caused by the flood wave are not equal in time and differ per location in the system. Table 5.1 indicates the locations most vulnerable for flooding, the locations are visualized in Appendix Figure H.1. The height maps indicating the flood locations are also presented in Appendix H.

Location	Canal\River	Levee height
Side Canal B & C	NSC	+0.40 m NAP
Westpoort	NSC	+0.85 m NAP
Houthavens	NSC	+0.80 m NAP
Central Station Amsterdam	NSC	+0.85 m NAP
Weesp	ARC	+0.65 m NAP
Kuijerpolder	Vecht	+0.35 m NAP
Polder near Houten	ARC	+0.60 m NAP

Table 5.1: Critical locations flooding

5.3. Economical Effect

The economical effect resulting from flooding is a difficult parameter to define. Available literature links the specific water levels on the canal to a roughly estimated damage cost (De Beland et al., 2016). The water levels, sources of the damages and the costs described by the literature are stated in Table 5.2.

The literature used the assumption of a parabolic relation between the water levels on the canal and the costs of damage.

Water level canal [... m NAP]	Damage source description	Costs of damage [€]
-0.30	Request to limit discharging from the polders	75 000
-0.20	Water flows in sewage system Amsterdam, IJfront is closed and disconnected	300 000
-0.10	Problems with water management Vecht around Utrecht	1 600 000
0.00	Pumping stop to all polders	101 600 000
0.10	- Not specified -	200 000 000
0.20	- Not specified -	500 000 000
0.30	- Not specified -	1 000 000 000

Table 5.2: Damages according ROBAMCI 2016 (De Beland et al., 2016)

To estimate the damage per specific water level, the data from De Beland et al. (2016) is interpolated parabolically. This interpolation is visualized in Figure 5.2.

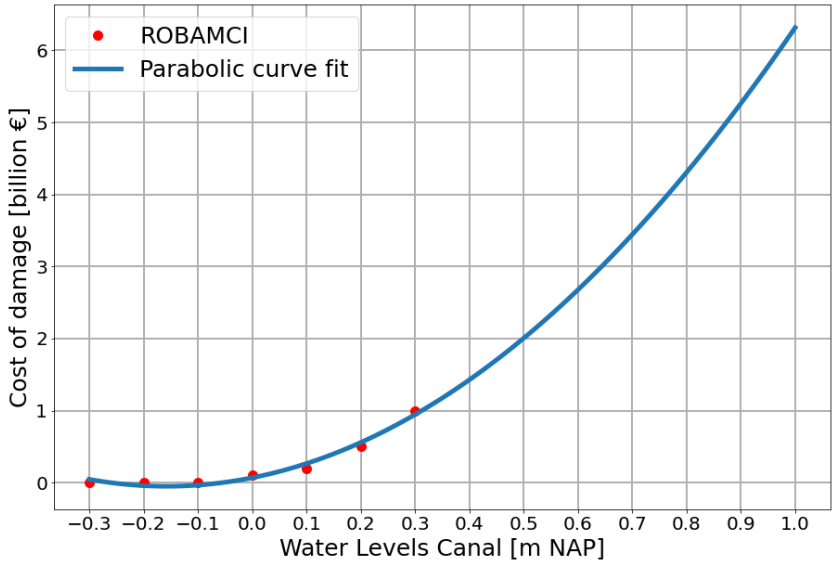

Figure 5.2: Parabolic interpolation of the damage costs

The method presented by De Beland et al. (2016) has its limitations that need to be mentioned, putting the method into perspective of this research. The method is based on a single water level spread out over the NSC and ARC, however due to the behavior of the flood wave, there is no equal water level present on both the canals. Water levels strongly differ between both the different canals and along the same canal. Therefore, it is hard to link costs of damage to a single water level. Another difference with the De Beland et al. (2016) method is that the damages due to the flood wave are only caused by the peak of the flood wave. The maximum water levels are reached for a short duration of time. Therefore, damages due to flood wave induced high water are limited. Similarly, the volume of water able to overtop the levees is limited for the same reason. For these reasons, it is expected that the costs of damage presented by De Beland et al. (2016) are overestimated by the described parabolic relationship.

In Appendix H the costs of damage as a result of a certain water level in the critical flood areas is calculated with a module of Rijkswaterstaat (IPLO, 2024). This estimation for the cost of damage serves as a rough guideline for the damages due to flooding of the critical flood areas and is presented in Table 5.3. This guideline also supports the assumption that the De Beland et al. (2016) method is overestimating the costs of damage. More research is needed on the relationship between the flood wave induced water levels and the corresponding costs of damage for the water system. In this research, the overestimated damages of De Beland et al. (2016) are used to determine the costs of damage needed for the final risk assessment.

	Levee height [m NAP]	**Water level in area [m]**	**Area [km^2]**	**Total inflowing volume [m^3]**	**Damage**	**Residents**	**Casualties**
Zijkanaal B en C	+0.40	0.01	4.30	43 000	€ 610 000	229	0
	+0.40	0.10	4.30	430 000	€ 6 000 000	229	0
Houthavens	+0.80	0.01	0.18	1 800	€ 1 300 000	3058	0
	+0.80	0.10	0.18	18 000	€ 13 000 000	3058	0
AMS Central Station	+0.85	0.01	0.07	700	€ 300 000	0	0
	+0.85	0.10	0.07	7 000	€ 3 000 000	0	0
Westpoort	+0.85	0.01	0.90	9 000	€ 3 600 000	76	0
	+0.85	0.10	0.90	90 000	€ 36 000 000	76	0
Weesp	+0.65	0.01	2.70	27 000	€ 8 600 000	11490	0
	+0.65	0.10	2.70	270 000	€ 84 000 000	11490	1
Kuijerpolder	+0.35	0.01	2.40	24 000	€ 730 000	1329	0
	+0.35	0.10	2.40	240 000	€ 7 200 000	1329	0
Houten polder	+0.60	0.01	1.20	12 000	€ 75 000	8	0
	+0.60	0.10	1.20	120 000	€ 740 000	8	0

Table 5.3: Damage due to inflow of canal water

The costs of damage are determined for the different maxima on the canal for every storms scenario with the use of the interpolation. For the 3 different failure durations, the results for the selected storms are presented in Table 5.4.

Scenario	3h spill Failure		6h spill Failure		12h spill Failure	
	h_{max} [m]	Costs [million €]	h_{max} [m]	Costs [million €]	h_{max} [m]	Costs [million €]
1	-0.036	20	0.149	397	0.152	405
2	-0.030	27	0.178	485	0.191	527
3	-0.015	46	0.262	787	0.378	1313
4	-0.014	48	0.282	868	0.409	1475
5	0.006	77	0.343	1140	0.575	2500
6	0.023	105	0.344	1145	0.500	2005
7	-0.004	62	0.393	1390	0.859	4860
8	-0.042	13	0.393	1390	0.862	4889

Table 5.4: Damages for Amsterdam Surinamekade

Due to the earlier mentioned limitation for the failure of 3 hours and unlikeliness of the 12 hours during failure scenarios, the final risk determination is based on the 6 hours during spill failure. For the 6 hours of failure, all possible storms are generated by combining all the different storm parameters according Table 3.6. For all these storms the maximum water level at the location: Amsterdam Surinamekade is calculated with the model. When the storm does not have a spilling window at the beginning of the storm, the water level at the canal remains at -0.40 m NAP. In Appendix G the results for the storms are presented. The probabilities per storm event are generated by multiplying the probabilities: P_{setup}, P_{φ} and P_{tide}, as already discussed in Section 3.2.2.

The yearly exceedance frequency of high water in the North Sea Canal as a result of the spill failure is depicted in Figure 5.3. These yearly water level frequencies are based on the model data for 6 hours of spill failure.

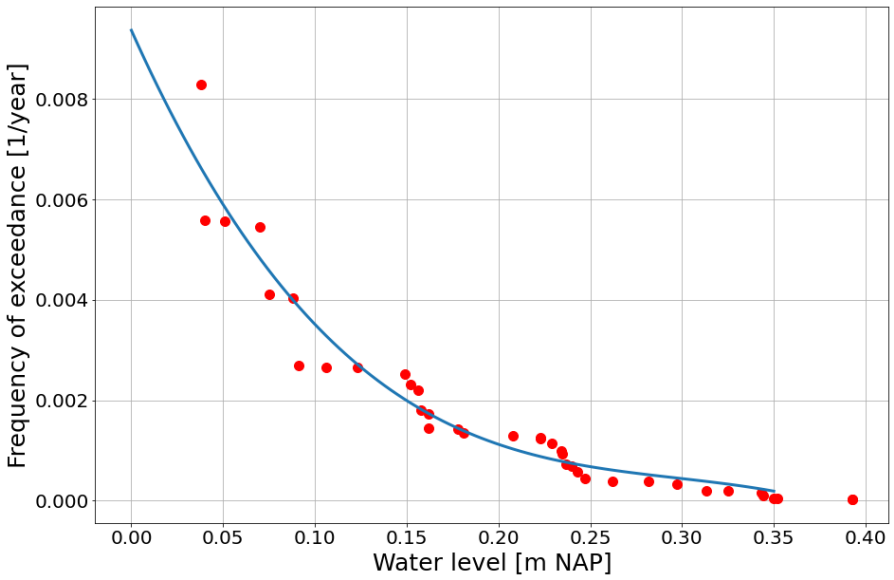

Figure 5.3: Exceedance frequency for high water on the NSC

For every storm, the maximum water levels at Amsterdam Surinamekade are linked to the costs of damage with the estimation method used by the De Beland et al. (2016). Figure 5.4 presents the relationship between the costs of damage and the return period of these damage costs. The blue line is a curve fit for the red dotted calculated values.

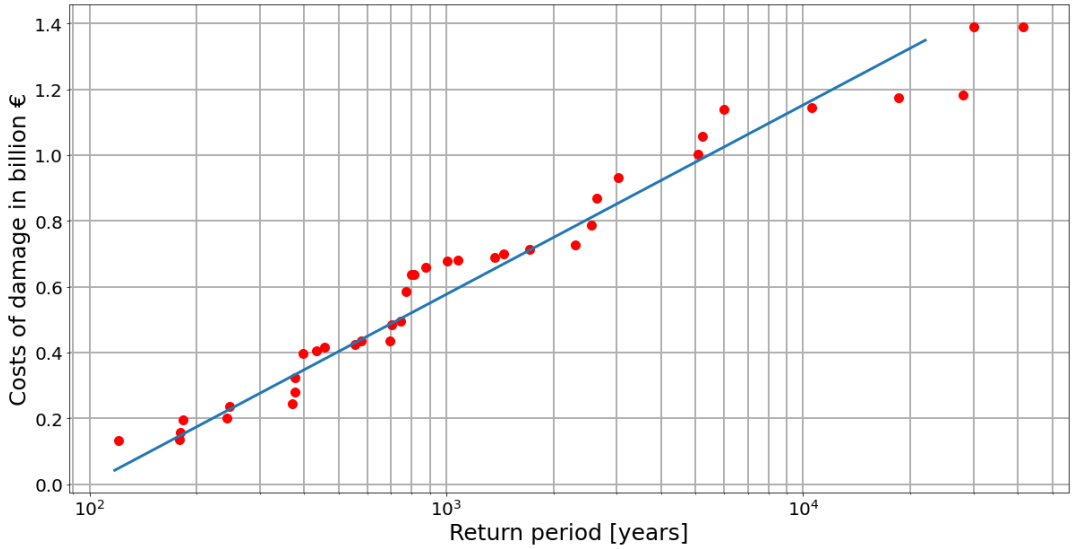

Figure 5.4: Return period for the cost of damage

The total flood risk is calculated by multiplying the costs of damage with the probability for each storm. Performing this calculation for all storms and adding the individual storm risks, results in the total risk for spill failure of 6 hours. The risks per storm are presented in Appendix G. The total flood risk for all storm scenarios is: €145 850 000,-. This probability is multiplied with the yearly probability of non-closure of the spill, determined in Section 3.2.1. The final estimated increased flood risk as a result of 6 hours of spill failure is: **€2 625 000,-** per year.

6

Discussion

This chapter discusses the results obtained from this research. The differences between the results of the spill failure and the ship lock failure (Middensluis) are compared. Furthermore, the influence of the storm duration on the shape of the storm, as well as the resulting effects on the flood wave are discussed. The outcomes of the research are also compared to the legal assessment. Finally, the main limitations of the research are identified.

6.1. Difference between Spill and Ship Lock Failure

The failure mechanism that is most critical for flooding of the water system is failure of non-closure of the spill gates. The effects on the water system as a result of ship lock failure is considered to be within acceptable limits. Only for the Middensluis the expected return period is low enough to be reviewed in this research.

Based on the modeled results for an extreme storm scenario, the impact due to failure of the Middensluis is considered to be low, especially when compared to the effect of non-closure failure for the spill gates. The extreme storm in combination with non-closure of the Middensluis outer head resulted in a maximum water level in the canal of: -0.05 m NAP. This water level is not exceeding the extreme high water level of +0.00 m NAP. For 6 hours of spill failure, the water levels do exceed this value and the water reaches a maximum of +0.35 m NAP. The reason for the difference between the two failure scenarios is further discussed in the coming section.

First of all, there is a difference in inflow for both failure events. The flow through the spill is primarily governed by the head difference between the sea and canal. The tidal motion of the sea alone already contributes to a significant inflow through the spill tubes. During neap tide, the maximum modeled flow through the spill is 630 m^3/s. Additionally, the combined flow area of all seven spill tubes is almost 200 m^2. During ship lock failure, the inflow is mainly determined by the exceeding sea height above the retaining height of the inner head. Only the peak of the storm is able to enter the water system. The modeled flow over the lock is at maximum: 125 m^3/s. Although the inflow of water over the lock persist for longer duration during the extreme event, the total inflow remains significantly lower than the total inflow through the spill. The flow area over the lock is dependent on the constant width of 25 meter, but also on the variable head over the lock. This flow area is considerably lower than for spill flow.

The low retaining height of the inner head of the Middensluis appears to be susceptible for large inflow of water during failure, however the modeled results indicate that spilling failure is significantly more critical. The suggested strategy to lower the canal level in case a large storm is forecast will create a buffer in the canal to prepare for potential failure due to non-closure of the outer head of the Middensluis. The advantage with failure of the Middensluis is that it only occurs in combination with large storms that are forecast. While spill failure is not depending on storms, as the tidal cycle will already provide considerable inflow. This makes spill failure more unpredictable.

6.2. Duration of Spill Failure

The maximum height and duration of the storm determine the shape of the storm. In Figure 6.1, two storms are visualized with an equal maximum storm height, however with two different durations of storm. The storm with a smaller duration does rise faster in water level $\theta_1 > \theta_2$. This storm behavior will cause a higher inflow into the system at the begin stadium of the storm. As the spill failure only takes 3, 6 or 12 hours, this begin stadium of the storm is critical. With more extreme storms it is expected that there is no spill window at the start of the storm, or that the duration of the storm is high enough to prevent fast water rise at sea in the begin stadium of the storm. The most unfavorable storm for spill failure has a high maximum water level in combination with a low total storm duration.

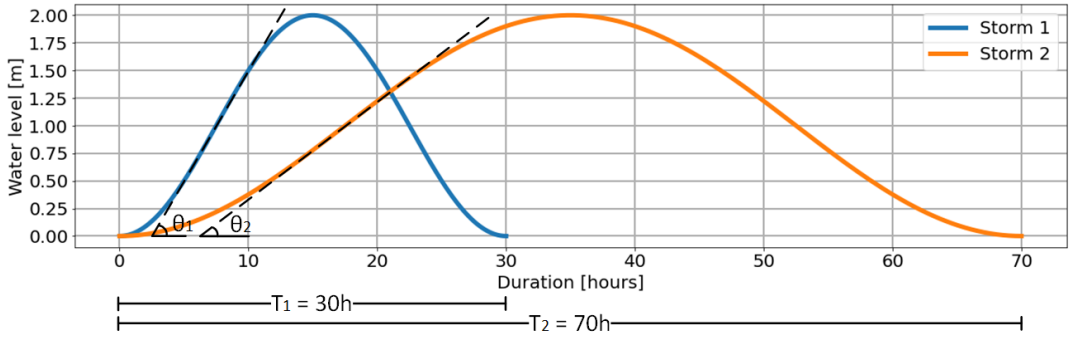

Figure 6.1: Comparison between two storms with different storm durations

For a short 3 hour duration of failure, the inflow is largely dependent on the shape of the storm. The results for 3 hours of failure demonstrate similar water levels in the canal, regardless of the maximum storm height. These similar water distributions are a result of the constant storm duration of 30 hours. During the first 3 hours, the storms is building up towards its maximum. After 6 and 12 hours, the results are differentiated based on the h_{max}.

The duration of failure is dependent on the time required to close the spill gates. Prior to this closure, some decisions and actions are to be taken. First of all, the unexpected rising of the water levels in the canal needs to be noticed. When this unconventional rise is observed, the cause for the water level rise needs to be found. When the opened spill gates are detected, a mechanic needs to be sent towards the spill complex to investigate the situation. In the end, the right actions result in the closure of the spill gates. The closure is always possible by releasing the doors manually, which causes the doors to slide into closed position by means of gravity. Whether failure happens during day or night time has an influence on the duration of the discussed processes.

6.3. Review Legal Assessment

With the conclusions drawn from this research, the assumptions and outcome of the legal assessment (Van den Berg et al., 2019), also mentioned in Section 1.2, are to be evaluated. The assumption that failure of the water system is described by the balance between incoming volume and the storage volume of the system does not adequately capture the dynamic behavior of an incoming flood wave. The flood wave induces continuously varying water levels throughout the water system, where the peak of the wave tends to cause local flooding. Furthermore, the legal assessment considers the failure of the spill gates to be negligible. The legal assessment states that the probability of opened spill gates can be assumed sufficiently small. After interpretation of this research, the probability of opened spill gates is not negligible. This research concludes that the biggest contribution to the flood risk of the water system comes from failure of the spill. The failure of the Middensluis is of minor influence when looking at the probability of occurrence and the corresponding effects on the water system. Therefore, the legal assessment should also incorporate failure of the spill as described in this research in the future.

6.4. Limitations

This section outlines the main limitations regarding this research. The first limitation concerns the calibration and validation of the model. The model is only calibrated with the measured data of the non-closure spill failure event on the 2nd of November 2023. Additionally, validation of the model is not possible due to the absence of more data, highlighting the effects of (spill) failure on the water levels in the canal. Furthermore, the calibration of the model for non-closure failure of the outer head of the Middensluis is not possible. The model is calibrated for spill failure, but also used for ship lock failure. Therefore, the modeled results of the water flowing over the lock gate cannot be directly compared with reality.

The model does not include the Vecht in the calculations for the water distributions in the water system. This exclusion was made due to the lack of detailed bathymetry data and the inability to calibrate and validate the model for the Vecht. The Vecht does not contain measurement locations representing the water levels during the failure event of the 2nd of November. The Vecht is contributing to the storage area of the water system, therefore the water levels, especially on the ARC, are expected to be slightly overestimated by the model.

The rate at which the target level in the water system is restored differs per situations. For instance, the volume of excess water in the polders determines the rate of water restoration on the canal. If high precipitation occurred during failure, the polders would contain a significant volume of excess water that must be discharged via the canal. This large volume of extra water results in more water to be discharged by the pumps and can result in longer duration of high water on the water system. Furthermore, different strategies and alternative pumps can be used to restore the water levels in the canals. This research mostly focuses on the maximum water levels as a result of failure, however it is important to note the difference between the model and reality.

Another limitation, previously discussed in Chapter 5, lies in the determination of the costs of damage due to high water on the canal. This determination is based on an estimation presented in literature (De Beland et al., 2016). This estimation focuses on high water in the canal as a result of insufficient discharge capacity of the pumps and spill at IJmuiden. However, this research focuses on high water as a result of a flood wave in the system, the key differences between the two failure mechanisms lie in the timescale and local variability. High water caused by the flood wave only lasts for one to one and a half days, whereas high water due to insufficient discharge capacity, is likely to happen for a longer period. Furthermore, the high water caused by the flood wave is constantly changing and varies locally. The maximum water levels in the canal are only reached during the peak of the flood wave.

Beland et al. (2016) describes the damage cost estimation method as getting a feeling for the damages due to the different high water levels in the canal. For a better cost estimation more research should be performed on the relationship between high water levels in the canal and the corresponding damages. Research on this relationship is out of the scope of this research. Therefore, the final risk calculations are performed to get an estimation for the final risk of failure for the spill. Taking into account that the flood wave only reaches maximum water levels for a limited amount of time, it is expected that the Beland et al. (2016) method overestimates the cost of damages. Follow-up research should prove whether this statement is valid.

7

Conclusion and Recommendations

This chapter concludes on the results obtained in the previous chapters. It provides a summary of the findings for every sub-question and answers the main research question. This chapter also provides recommendations based on the research results. The recommendations regard the spill-lock complex in IJmuiden, specifically focusing on the prevention of failure and the mitigation of the failure effects. Similar recommendations are provided for the responsible authorities for the entire water system.

7.1. Conclusion

The main research question is answered with the use of the following sub-questions, the answers for every sub-question are presented in this section:

1. **What are the relevant failure scenarios for the spill-lock complex, leading to entering of sea water into the water system?**
   The relevant failure mechanism for spill-lock failure is non-closure of all spill gates. Failure due to overtopping is considered irrelevant, as the return periods for the related extreme storms are exceeding the prescribed flood frequency of 1 in 10 000 years. Non-closure failure of the ship locks is only relevant for the Middensluis, as its inner head provides a very limited retaining capacity of +2.5 m NAP. The other ship locks provide sufficient retaining height on their inner heads. An extreme storm event was modeled for non-closure failure of the Middensluis. This simulation resulted in acceptable water levels on the canal. The extreme storm event combined with non-closure of the outer head resulted in a maximum water level of: -0.05 m NAP on the NSC with a return period of 833 333 years. Overtopping of the ship locks is also considered irrelevant due to the high return periods of corresponding extreme water levels.
2. **How does a flood wave evolve through the water system behind the spill-lock complex in IJmuiden?**
   The behavior of the flood wave on the canal is represented by the model. In the event of spill failure, the flood wave rises quickly towards +0.00 m NAP, within 3 to 4 at the NSC and 5 to 8 hours at the ARC. After 3 hours of failure, the canal water levels are not exceeding +0.00 m NAP and the relation between the storm pattern and the inflow is dominated by the duration of the storm. For 6 hours of failure, the maximum water levels on the canals range between +0.10 and +0.35 m NAP and the magnitude of the maximum storm levels determine the maximum levels on the canal. After 12 hours of spill failure, the maximum levels on the canals are between +0.10 m and +0.85 m NAP, however such an extreme storm event is considered unrealistic due to the long duration that all spill gates must remain opened. After closure of the spill gates a smaller wave is visible that resonates through the closed system. This internally resonating wave results in a variable pattern in the water levels.

3. **What are the consequences of the failure scenarios, due to their induced flood wave on the water system?**
   The economical costs of damage as a result of 6 hours spill failure events are between 132 and 1390 million euros. These costs are estimated based on a research (De Beland et al., 2016), providing a rough estimation for the relationship between the water levels at the canal and the costs of damage as a result of this high water. For every water level at the canal an estimation for the cost is generated. Damage can occur due to local flooding of agricultural land, the effects of a pumping stop on the polders, flooding of sewage systems, salinization, etc.

The main research question was formulated as follows:

What is the increased flood risk on the water system, North Sea Canal and Amsterdam Rhine Canal, as a result of inflowing sea water due to overtopping and non-closure failure of the spill-lock complex IJmuiden?
The increased flood risk as a result of the 6 hours during failure estimated to be **€2 625 000,- per year**. The flood risk per storm is obtained by multiplying the costs of damage with the probability of occurrence for every storm. In the end, all risks are summed and multiplied with the risk of non-closure of the spill gates. This calculation results in the total increased flood risk for the water system for 6 hours of spill failure.

7.2. Recommendations

In the line of this research some additional research can be performed to gather more useful information about the failure of the spill-lock complex IJmuiden. The storm duration needs to be varied, especially to see the effect on short duration of failures. The model could also be expanded with the addition of the side rivers Amstel and the Vecht. The Vecht can not be disconnected from the ARC, therefore the Vecht is also contributing to the total storage capacity of the system.

Another logical follow-up research should focus on the relationship between specific high water levels in the canal and the costs of damage of such water levels. This research is based on a rough estimation, while a more sound substantiation on the occurring costs of damage during failure is useful for the determination of the future maintenance and improvement strategy for the spill-lock complex and water system. Research linking the costs of damage to the high water levels at the canal is perfectly inline with this research, where the results of the model can be used to better specify the flood risk of the system.

It is important to raise awareness that the focus should not be limited to failure of the ability to discharge the water system only, but also on the retaining ability of sea water of the spill-lock complex. Most of the available research focuses on high canal levels due to insufficient discharge capacity. Noticing unexpected water level rise on the canal is most important, after which the failure cause needs to be located and addressed. When one or more spill gates are opened during high water at sea, this opening should be clearly reported to the operators at the control location. A control loop that is based on, for example, flow sensors in the spill tube, could confirm whether all spill gates are closed correctly. With the implementation of the control loop, failure can be noticed sooner, before sea water is able to flow into the system. When the spill gates are not closing, a mechanic can be send to the complex to identify the problem. The process of securing closure of the (outer) lock heads is similarly important for failure of the ship locks, however the non-closure of the outer head does not immediately result in failure, due to the retaining capacity provided by the closed inner head.

In case an extreme storm event is forecast, the water system could be prepared by discharging as much water out of the system and polders as possible. In case of failure due to non-closure of the spill or outer head of one of the locks, the system has an additional buffer to better sustain the increasing water level in the canal. With an extreme storm event the possibility of lock failure increases, especially if the inner head of the Middensluis is expected to be exceeded by the storm. Preparing the system for a predicted storm event is preferably done by using as much from the spill discharge capacity as possible. Therefore, it is important that the closure of the spill gates is confirmed just before the start of the storm event. Such a preparation of the system is less effective for spill failure as this failure is not depending on the presence of a storm.

In the event of a failure of the spill-lock complex, there are a few options to limit the effects on the water level. Once the failure cause has been addressed, the water system is required to return towards its target level. To limit effects on the water system, Rijkswaterstaat could further explore the possibility to incorporate the use of its fresh water lakes located along the system. For example, via the Oranjes-luizen at the connection between the NSC and the Markermeer water can be discharged onto the lake. The Markermeer is usually between -0.40 and -0.10 m NAP and can be used for discharging as long as the water level at the NSC is above the level of the Markermeer. The Markermeer has a very big storage capacity compared to the water system. Therefore, the water levels on the Markermeer are not expected to rise drastically. Another option is the use of other pumping stations present along the system, such as the Zeeburg pumping station.

The Vecht is also connected to the Markermeer with the locks at Muiden. These locks can also be used to decrease the water level in the Vecht. Numerous fresh water lakes located along the Vecht can be used for temporary storage of excess water levels. These measures would significantly increase the total storage area of the system and therefore, lower the water levels along the system. Due to the large surfaces of the lakes, the influence on the lake water levels is expected to be small. Nonetheless, research should be performed on the intrusion of saline water in the system during failure, as this intrusion effect the state of the fresh water lakes and drinking water facilities, which is unfavorable.

Contrary to above mentioned strategy, the decision can be made to reduce the water level in the water system by disconnecting the Vecht similarly to the Amstel. Most critical damage locations are along the Vecht. Similar to the disconnection of the Amstel from the NSC and ARC, the Vecht could also be disconnected from the ARC. This disconnection would protect the Vecht from unfavorable high water levels in the river. The disconnection is only helpful when the water levels at the rest of the water system are not raising too high as a result of the loss of part of the storage area. The consideration can be made to use the Vecht until a certain water level, after which it is disconnected from the ARC, to prevent further rising on the Vecht, while still maintaining part of the storage capacity of the Vecht. All regional retaining structures and levees should be checked regularly on their ability to retain at their maximum capacity. These checks can prevent undesirable surprises when retaining of high water in the canal is expected.

References

AHN. (2022). *Actueel Hoogtebestand Nederland* (tech. rep.).

Bakker, A., Rovers, D., & Mooyaart, L. F. (2025). Storm Surge Clusters, Multi-Peak Storms and Their Effect on the Performance of the Maeslant Storm Surge Barrier (The Netherlands). *Journal of Marine Science and Engineering*.

Biscarini, C., Di Francesco, S., & Manciola, P. (2010). CFD Modelling Approach for Dam Break Flow Studies. *Hydrology and Earth System Sciences*, *14*(4).

Chbab, H. (2017). *Basisstochasten WBI-2017: Statistiek en Statistische Onzekerheid* (tech. rep.). Deltares.

De Beland, M., Klanker, G., Klerk, W., Wessels, J., Van der Wiel, W., De Wit, A., Jansen, T., & Sminia, M. (2016). ROBAMCI: Case Kunstwerken - Gemaal IJmuiden.

Hill, P., Bowles, D., Nathan, R., & Herweynen, R. (2002). On the Art of Event Tree Modeling for Portfolio Risk Analyses. *Ancold Bulletin*, 99–108.

Hydrologic. (2021). *Vervolg Kosteneffectiviteit ARK-NZK* (tech. rep.). Rijkswaterstaat WVL.

Hydrologic. (2022). *Slim Watermanagement Redeneerlijnen Amterdam-Rijnkanaal Noordzeekanaal* (tech. rep.). Rijkswaterstaat and Water Boards.

Informatiepunt Leefomgeving (IPLO). (2024). Schade- en Slachtoffer Module [Version 4.2.0 [Computer software]]. *Rijkswaterstaat*.

Jongejan, R., & Maaskant, B. (2013). Applications of VNK2, a Fully Probabilistic Risk Analysis For All Major Levee Systems in the Netherlands. *In: Comprehensive Flood Risk Management. Taylor & Francis Group, London*.

Koedijk, O. (2020). *Richtlijnen Vaarwegen 2020* (tech. rep.). Rijkswaterstaat Dienst Water, Verkeer en Leefomgeving.

Kok, M., Van Berchum, E., & Strijker, B. (2021). Quickscan Zeespiegelstijging Amsterdam: Verkenning naar de Invloed van Zeespiegelstijging op Water en Ruimte in Amsterdam.

Kuijper, B., & Geerse, C. (2016). *Doorontwikkeling DEZY 2.0* (tech. rep.). HKV Lijn in Water.

Lendering, K., Schweckendiek, T., & Kok, M. (2018). Quantifying the Failure Probability of a Canal Levee. *Georisk: Assessment and Management of Risk for Engineered Systems and Geohazards*, *12*(3), 203–217.

Lewin, J., Ballard, G., & Bowles, D. (2003). Spillway Gate Reliability in the Context of Overall Dam Failure Risk. *USSD Annual Lecture*, 1–17.

Ministry of Infrastructure and Water Management. (2025). Water Act. https://wetten.overheid.nl/BWBR 0025458/2024-01-01

Mooyaart, L., Bakker, A., Van den Bogaard, J., Jorissen, R., Rijcken, T., & Jonkman, S. (2025). Storm Surge Barrier Performance—The Effect of Barrier Failures on Extreme Water Level Frequencies. *Journal of Flood Risk Management*, *18*.

Mooyaart, L., Bakker, A., Van den Bogaard, J., Rijcken, T., & Jonkman, S. (2023). Economic Optimization of Coastal Flood Defence Systems Including Storm Surge Barrier Closure Reliability. *Journal of Flood Risk Management*, *16*.

Neelen & Schuurmans. (2006). *Boezemsysteem Amstel, Gooi en Vecht: Hydraulische Analyse* (tech. rep.).

Peramuna, P., Neluwala, N., Wijesundara, K., DeSilva, S., Venkatesan, S., & Dissanayake, P. (2024). Review on Model Development Techniques for Dam Break Flood Wave Propagation. *Wiley Interdisciplinary Reviews: Water*, *11*(2).

Rijkswaterstaat. (2014). *Vervangingsopgave Natte Kunstwerken* (tech. rep.).

Rijkswaterstaat. (2024). Water Info [Accessed: 2024]. https://waterinfo.rws.nl/nav/bulkdownload/

Salmasi, F., & Abraham, J. (2023). *Hydraulic Performance of Sluice Gates: A Review of Head Loss Estimation and Discharge Coefficients for Optimal Flow Control and Design Considerations* (tech. rep.). Intechopen.

Saman, K. (2017). *Prestatiepeilenmodel Oosterscheldekering 2017* (tech. rep.). RWS Zee en Delta District Noord.

t' Hart, R. (2018). *Fenomenologische Beschrijving, Faalmechanismen WBI* (tech. rep.). Deltares.

Triki, A. (2017). *Further Investigation on the Resonance of Free-surface Waves Provoked by Floodgate Maneuvers: Negative Surge Waves* (tech. rep.). Ocean Engineering.

Van Beekvelt, B., De Buisonje, B., Veenman, R., Haan, J., & Van der Sande, R. (2022). *Waterakkoord Noordzeekanaal en Amsterdam-Rijnkanaal* (zaak 31172855) (Signed on: 13 October 2022). Rijkswaterstaat, Water Board Amstel Gooi en Vecht, Water Board Hollands Noorderkwartier, Water Board De Stichtse Rijnlanden, and Water Board van Rijnland.

Van den Berg, S., Casteleijn, A., Tánczos, I., Kruis, M., Noordman, B., Osmanoglou, D., & Plomp, I. (2019). *Wettelijke Beoordeling Dijktraject 44-3 IJmuiden* (tech. rep.). Ontwerpbureau Rijkswaterstaat.

Wang, B., Zhang, J., Chen, Y., Peng, Y., Liu, X., & Liu, W. (2019). Comparison of Measured Dam-break Flood Waves in Triangular and Rectangular Channels. *Journal of Hydrology*, *575*.

Winter, H. (2011). *Effecten van Gemaal IJmuiden op de Uittrek van Schieraal: Integratie van de Onderzoeken tijdens de Periode 2007-2011* (tech. rep.). Institute for Mariner Resources & Ecosystem Studies.

Zethof, M., Jansen, M., Van den Berg, B., Knops, D., & Stijnen, J. (2023). *Systeemanalyse Waterveiligheid: Deelrapportage Harde Waterkeringen Kust* (tech. rep.). HKV lijn in water and Witteveen & Bos.

A

Research Path

This Appendix presents the enlarged version of the research path that is mentioned in Section 1.6.

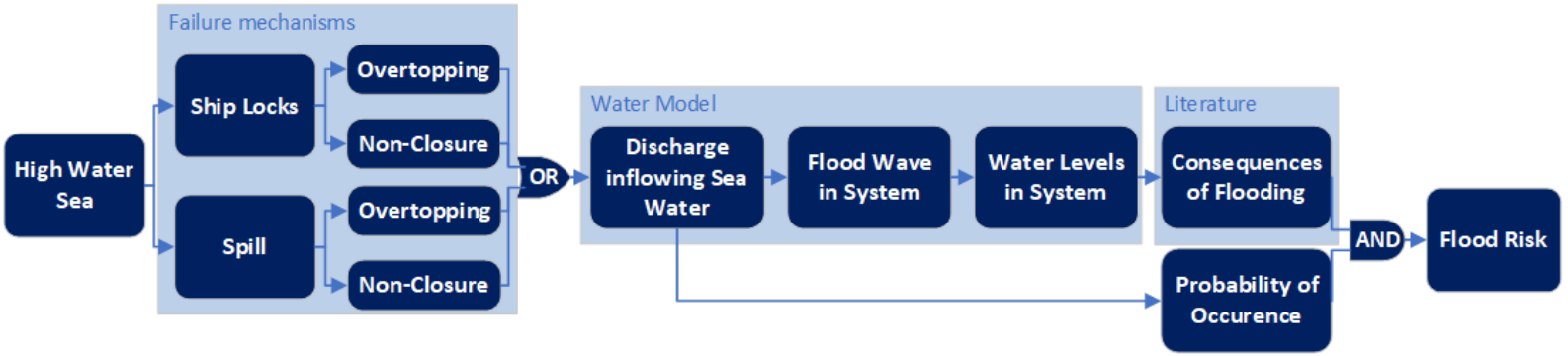

Figure A.1: Research path (enlarged)

B

Water Boards in the System

There are four water boards that depend on the water system for the discharge of the polders.

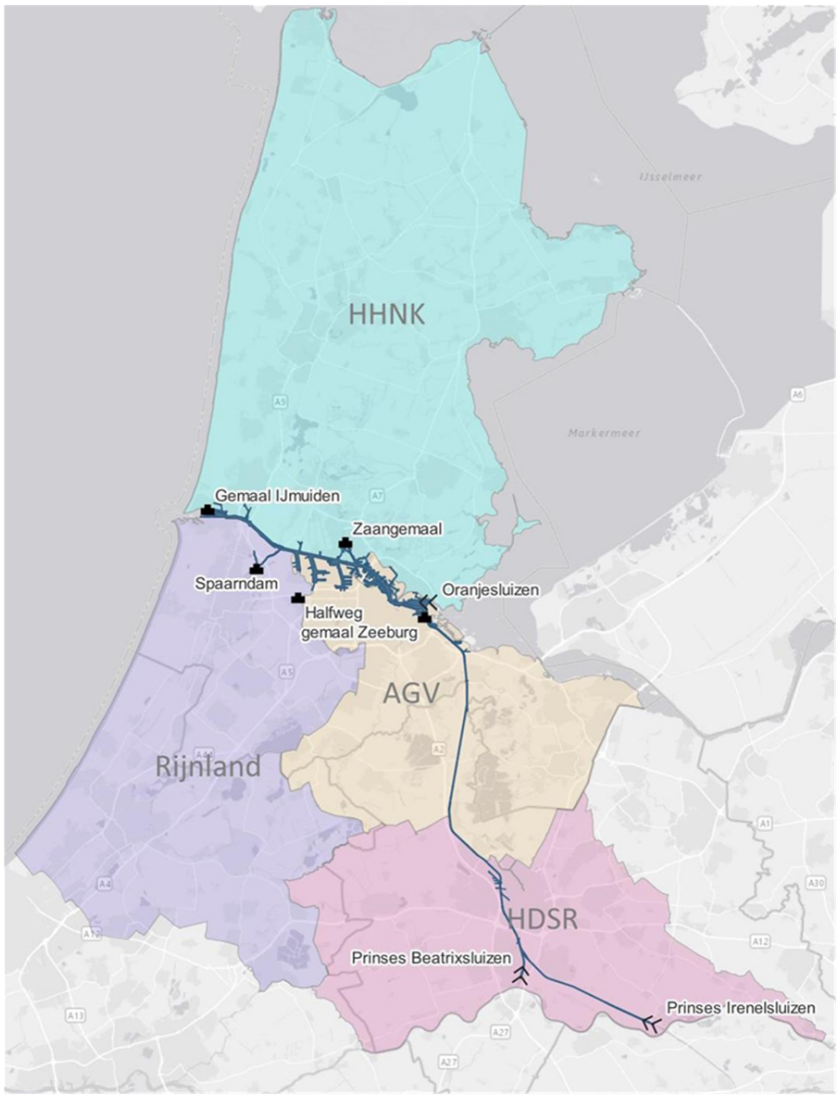

Figure B.1: Water boards in the water system (Hydrologic, 2022)

C

Geographical Background of the Water System

This Appendix presents the water system consisting of the main canals, side rivers and basins. Also the location of the pumps and ship locks present in the water system are indicated. The system contains 116 local pumping stations and 51 ship locks, varying in size.

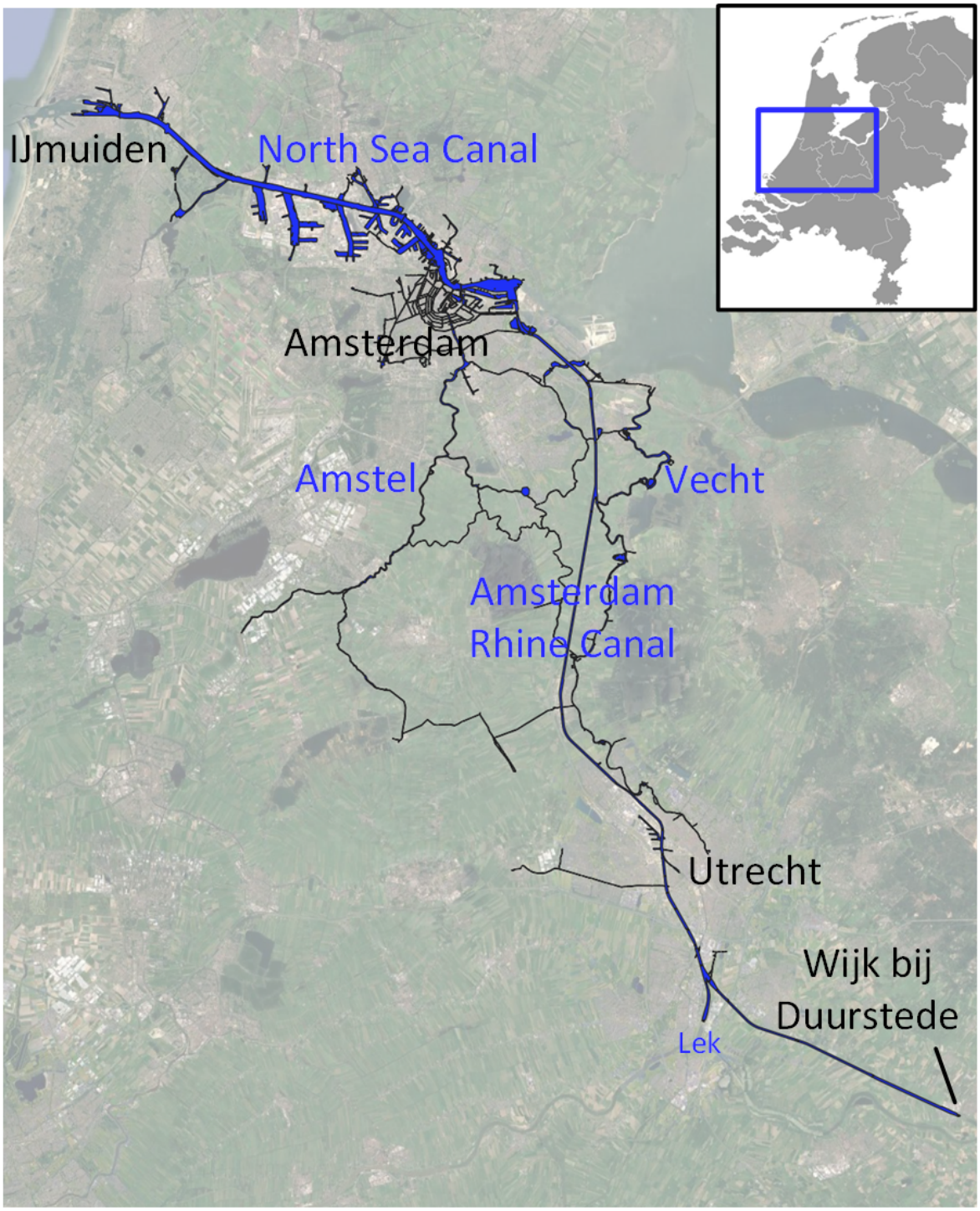

Figure C.1: Geographical position of the water system

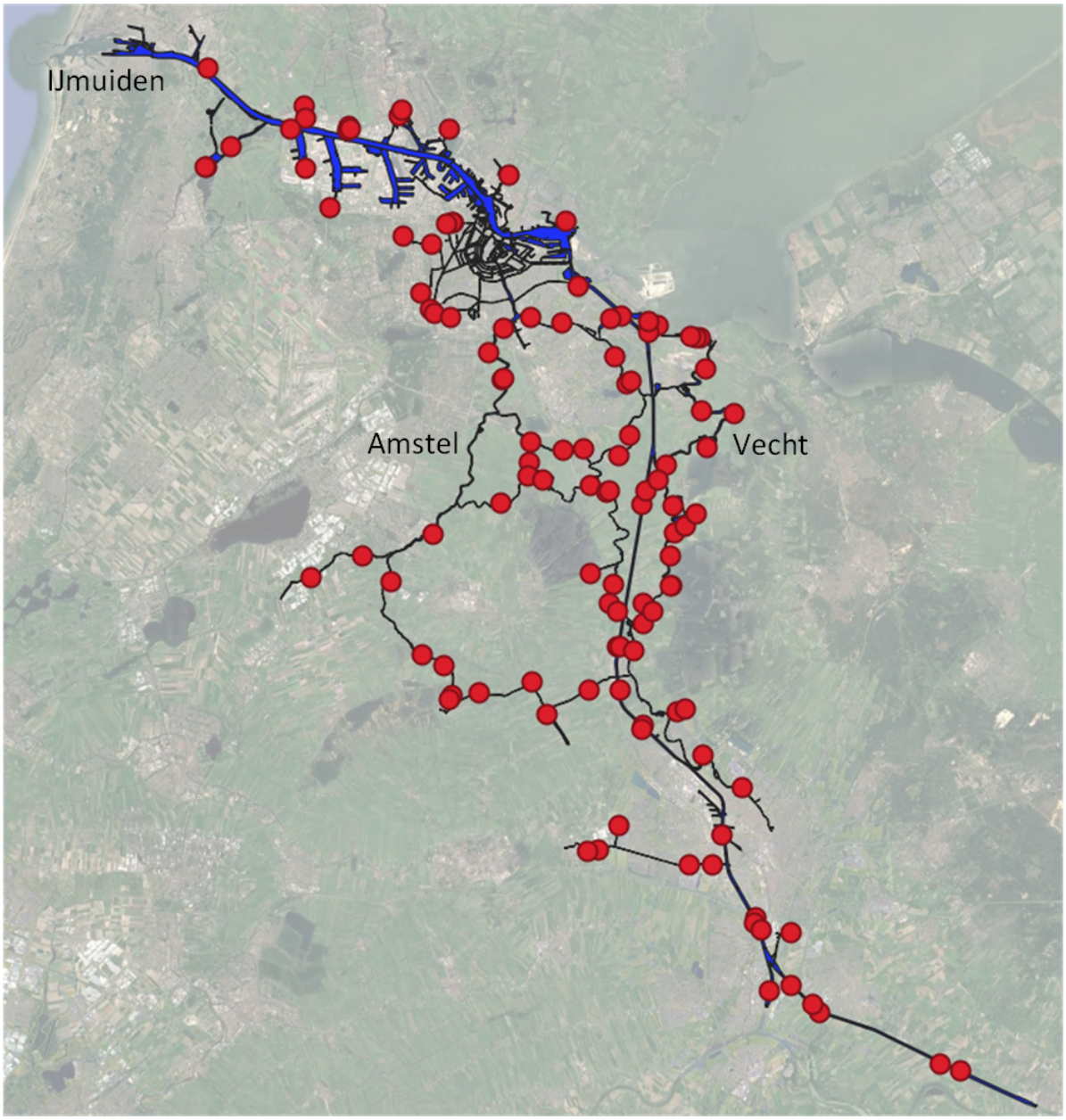

Figure C.2: Location of pumping stations in the water system

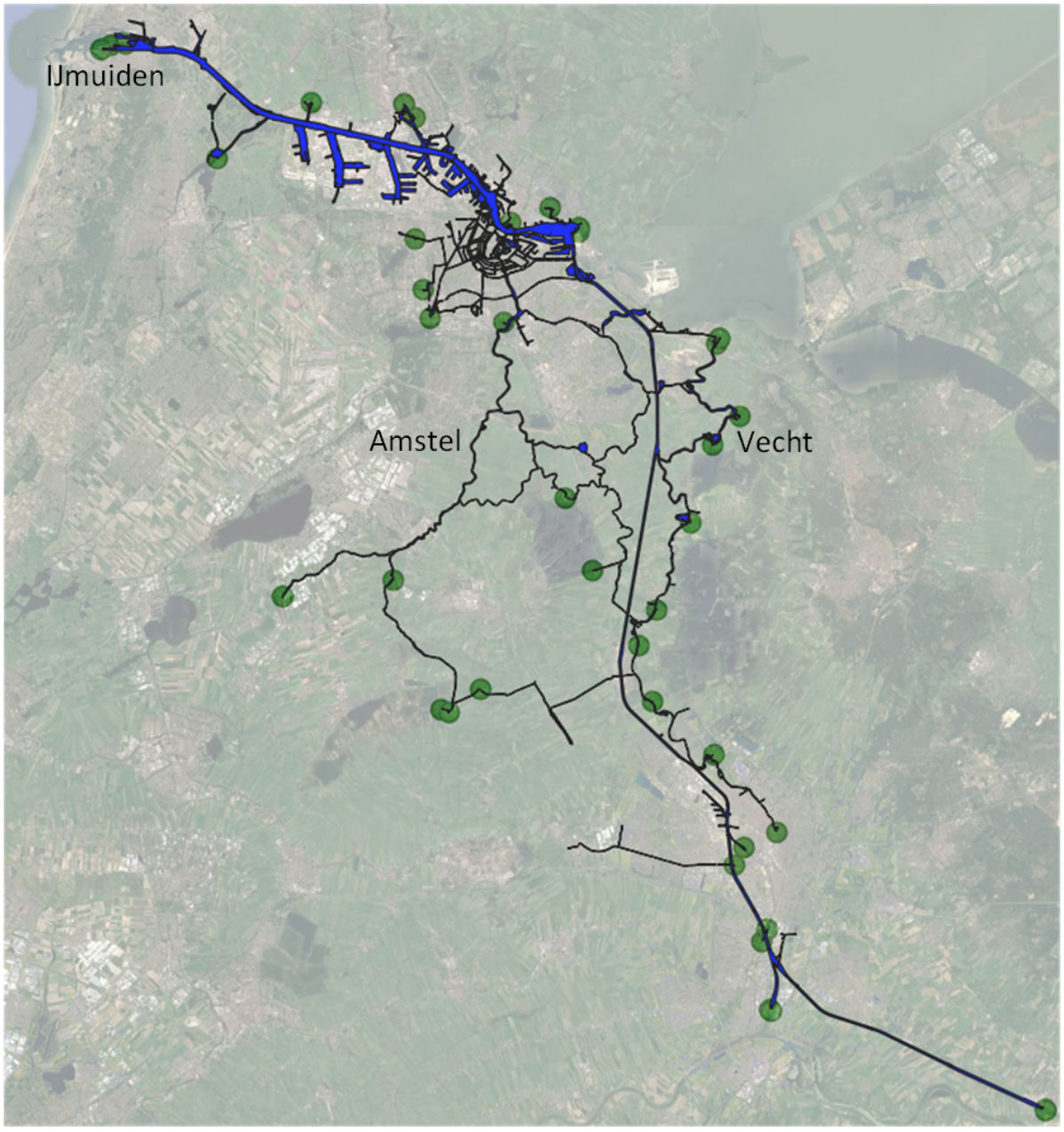

Figure C.3: Location of ship locks in the water system

D

Bathymetry NSC and ARC

This Appendix presents the bathymetry of the North Sea Canal and the Amsterdam Rhine Canal and its surroundings as is used for the model set-up and calculations.

Figure D.1: Bathymetry North Sea Canal

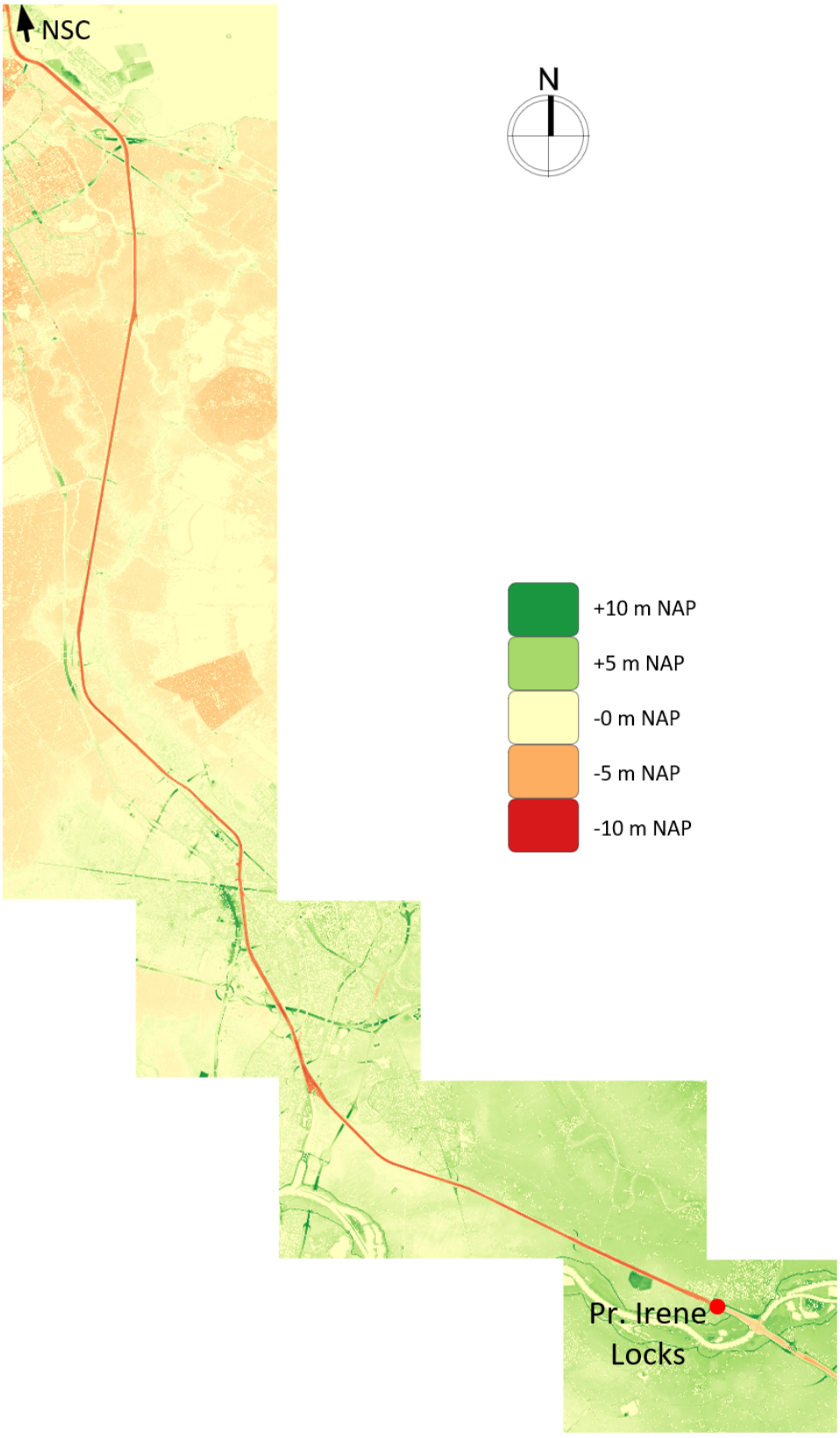

Figure D.2: Bathymetry Amsterdam Rhine Canal

E

Event Trees

The event trees per ship lock are presented in this Appendix.

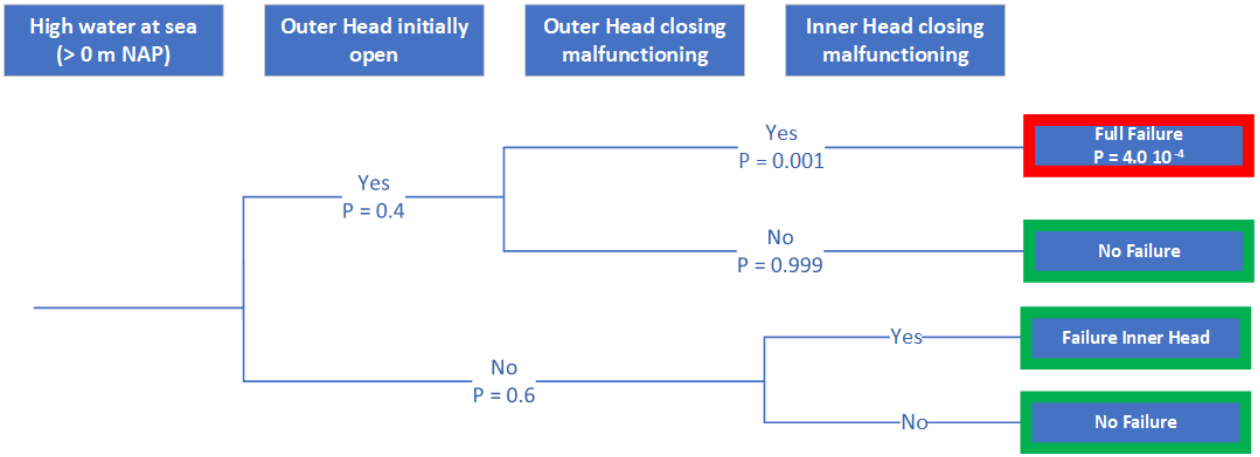

Figure E.1: Event tree Kleine Sluis

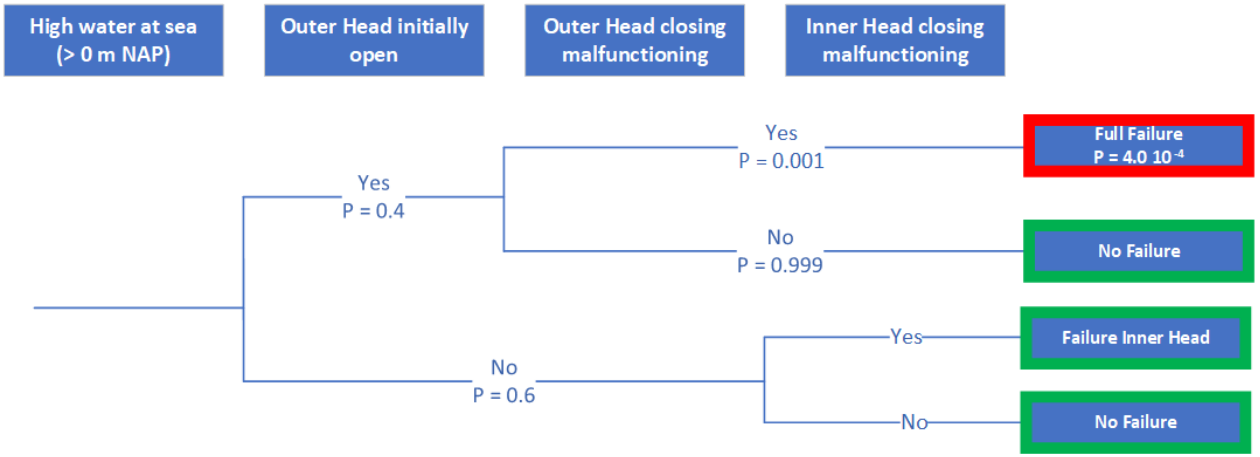

Figure E.2: Event tree Zuidersluis

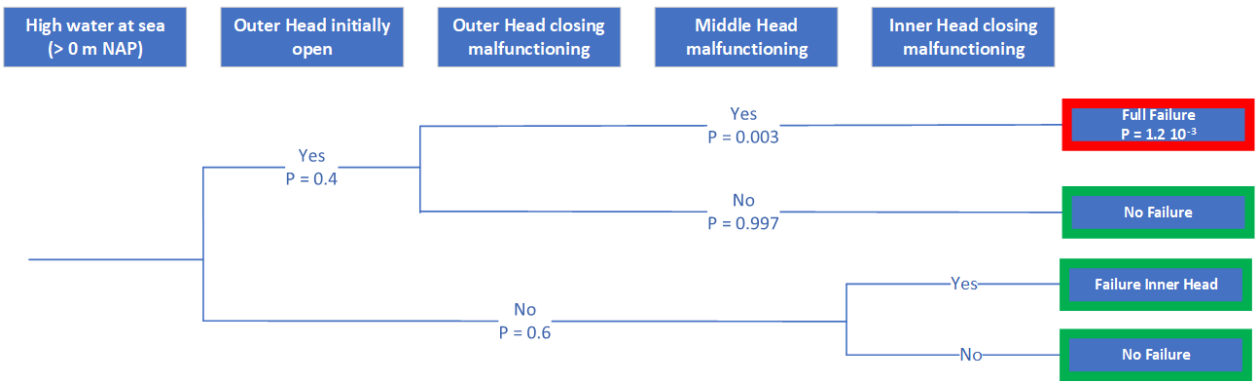

Figure E.3: Event tree Middensluis

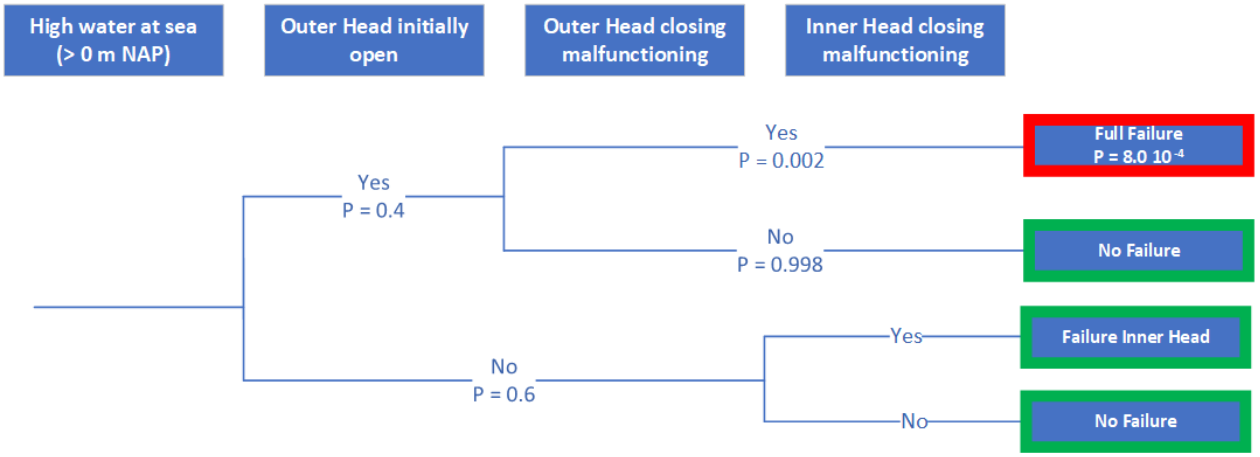

Figure E.4: Event tree Noordersluis

F

Model Results

This Appendix presents the model results enlarged as presented in Chapter 4.

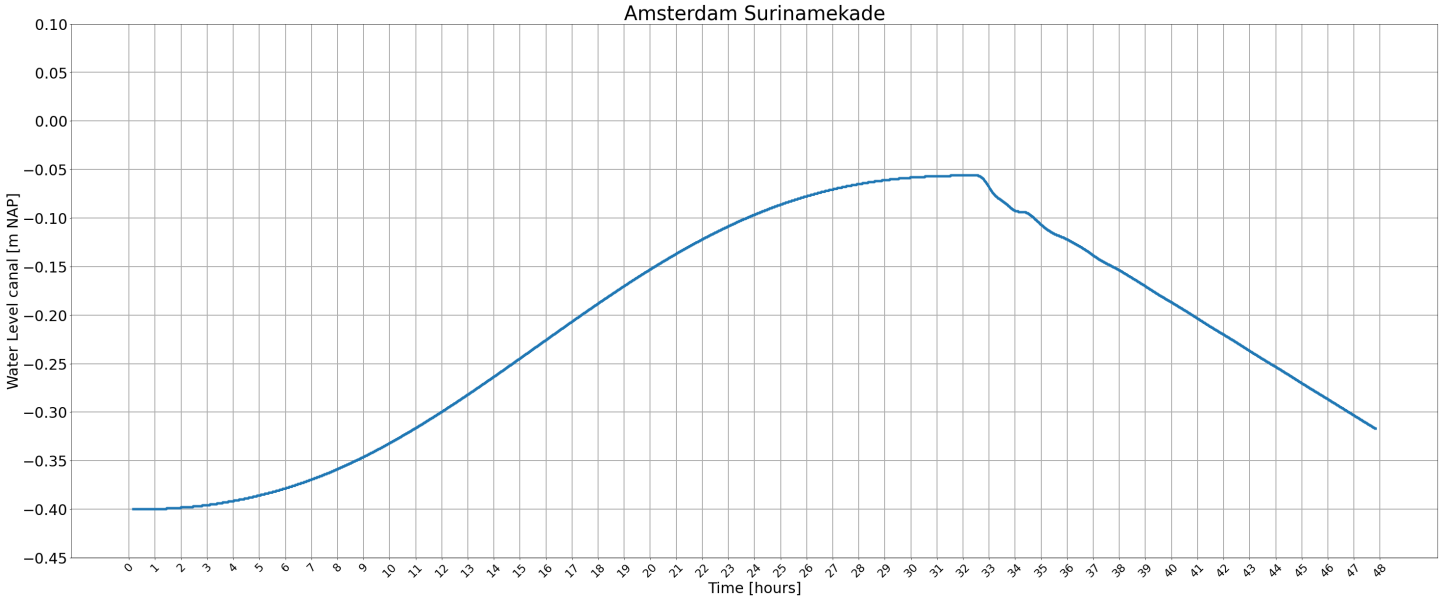

Figure F.1: Non-Closure of the outer head of the Middensluis

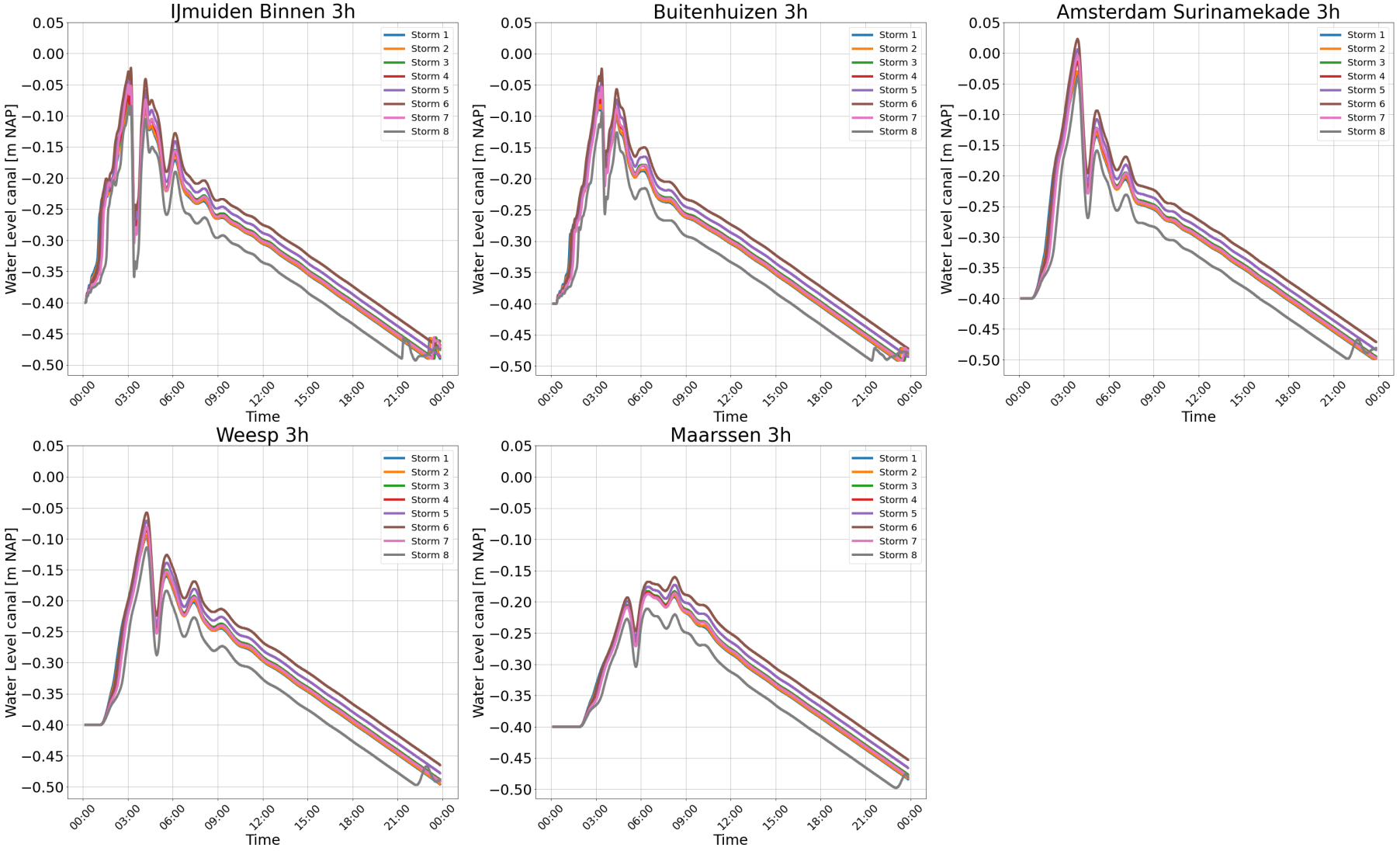

Figure F.2: Spill failure (3h) water levels on the canal

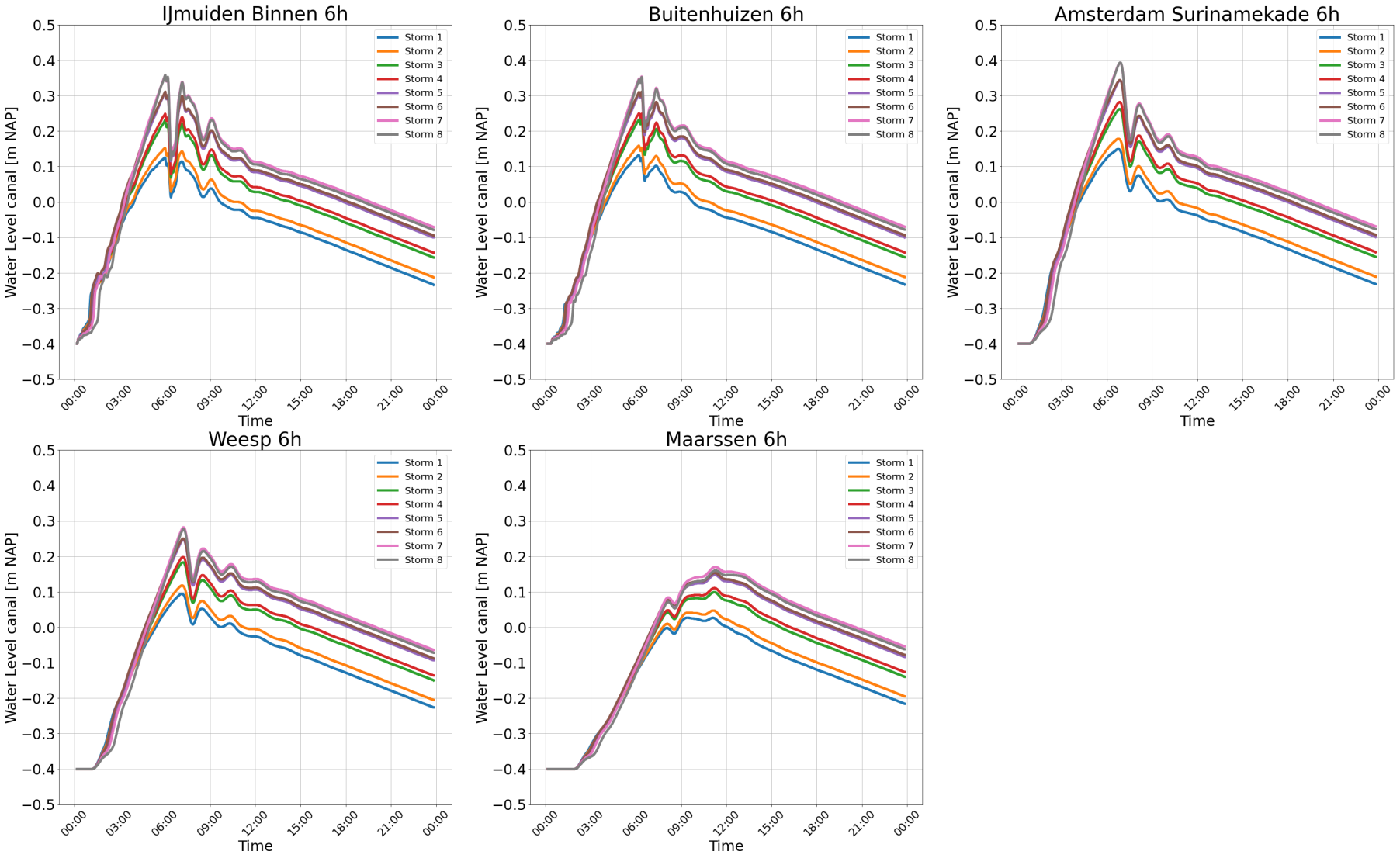

Figure F.3: Spill failure (6h) water levels on the canal

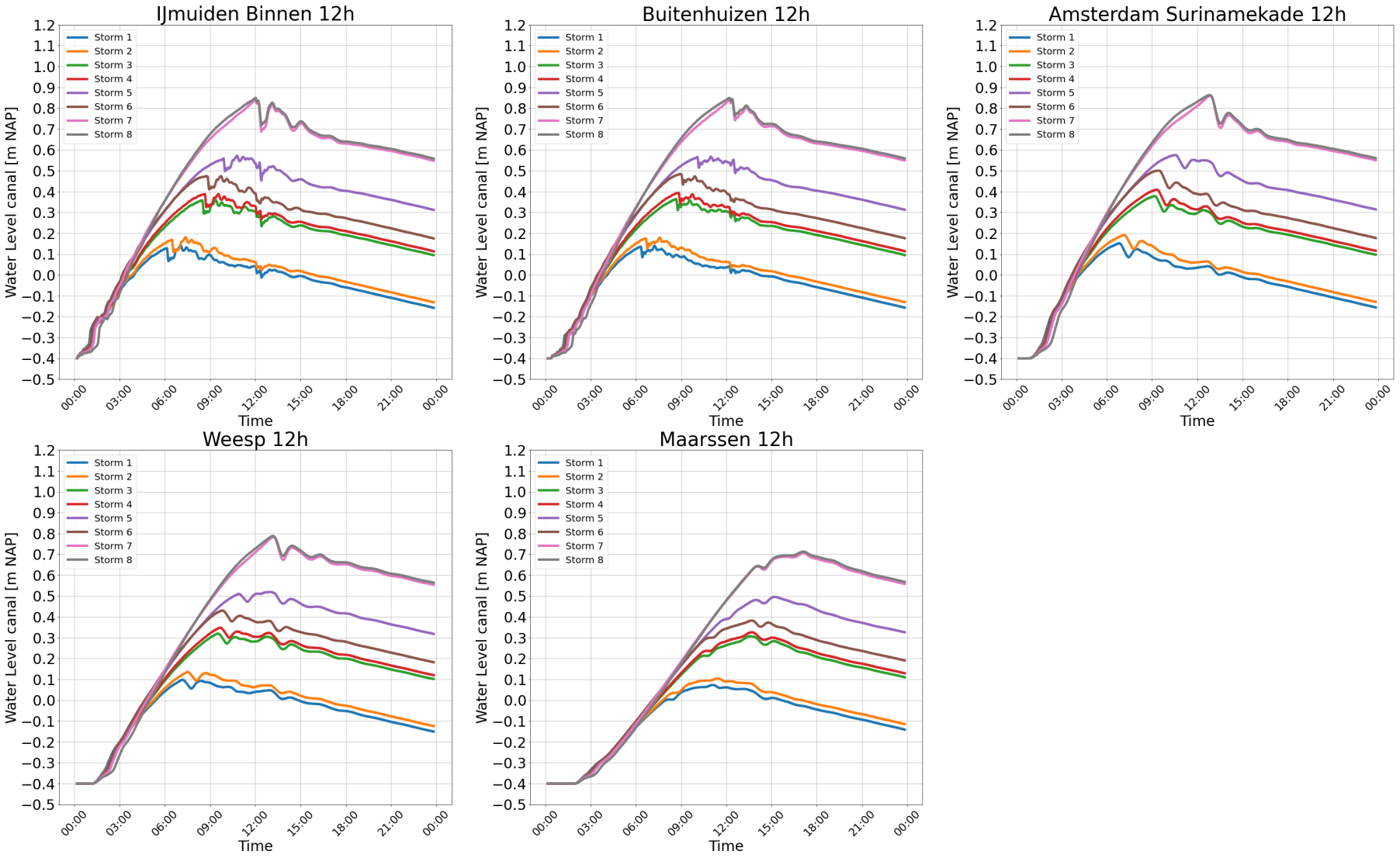

Figure F.4: Spill failure (12h) water levels on the canal

G

6h Failure Runs

This Appendix presents the results for the extra runs for the scenario of 6 hours of spill failure. The results for the filtered storms are presented in Table G.1. These scenarios cover the storms where a spilling window is present. All storms are presented in the tables in this Appendix.

h_{setup} [m]	φ	Tide	Probability	$h_{max,\ sea}$ [m]	$h_{max,\ canal}$ [m]	Costs million €
2.00	-6	intermediate	0.00013	2.20	0.393	1390
2.00	-5	intermediate	0.00050	1.99	0.393	1390
2.00	-4	intermediate	0.00103	1.78	0.352	1184
1.50	6	spring	0.00225	2.19	0.350	1174
1.00	6	spring	0.00399	1.86	0.344	1145
1.50	-5	intermediate	0.00137	1.73	0.343	1141
1.50	-6	intermediate	0.00035	1.89	0.325	1057
1.00	5	spring	0.00735	1.95	0.313	1002
1.50	-4	intermediate	0.00278	1.58	0.297	932
1.00	-6	intermediate	0.00063	1.59	0.282	868
1.00	-5	intermediate	0.00242	1.48	0.262	786
0.50	4	spring	0.00826	1.61	0.247	728
0.50	6	spring	0.00597	1.52	0.243	712
0.50	2	spring	0.00228	1.67	0.240	701
0.50	5	spring	0.01101	1.57	0.237	690
0.50	3	spring	0.00369	1.64	0.235	682
1.00	6	intermediate	0.00798	1.66	0.234	679
1.00	-4	intermediate	0.00493	1.38	0.229	660
1.00	-5	spring	0.00121	1.52	0.223	638
0.50	1	spring	0.00275	1.69	0.223	638
1.00	-4	spring	0.00247	1.41	0.208	585
1.00	-3	spring	0.00430	1.31	0.181	495
0.50	-6	intermediate	0.00094	1.28	0.178	485
0.50	4	intermediate	0.01651	1.41	0.162	435
0.50	-5	intermediate	0.00362	1.23	0.162	435
0.50	5	intermediate	0.02201	1.36	0.158	423
0.50	6	neap	0.00597	1.20	0.156	417
0.50	6	intermediate	0.01195	1.32	0.152	405
0.50	-4	intermediate	0.00738	1.18	0.149	396
0.50	-6	spring	0.00047	1.30	0.123	324
0.50	-5	spring	0.00181	1.25	0.106	280
0.50	-4	spring	0.00369	1.20	0.088	236
0.50	-3	spring	0.00644	1.15	0.070	196
0.50	-6	neap	0.00047	0.79	0.051	157
0.50	-5	neap	0.00181	0.74	0.038	132

Table G.1: Results from the 6 hour spill failure for all filtered storms

h_{setup} [m]	φ	Tide	Probability	$h_{max,\ canal}$ [m]	Damage costs €	Risk €
0.00	-	spring	0.075	0.091	243 441 000	18 258 000
0.00	-	intermediate	0.15	0.040	135 257 000	20 289 000
0.00	-	neap	0.075	0.072	200 249 000	15 019 000

Table G.2: Results from 6 hour spill failure for all storms (h_{setup} = 0.0)

h_{setup} [m]	φ	Tide	Probability	$h_{max,\ canal}$ [m]	Damage costs €	Risk €
0.50	-6	spring	0.00047	0.123	323 934 000	152 187
0.50	-6	intermediate	0.00094	0.178	485 007 000	455 721
0.50	-6	neap	0.00047	0.051	156 501 000	73 526
0.50	-5	spring	0.00181	0.106	279 961 000	507 323
0.50	-5	intermediate	0.00362	0.162	435 186 000	1 577 217
0.50	-5	neap	0.00181	0.038	131 518 000	238 326
0.50	-4	spring	0.00369	0.088	236 393 000	872 610
0.50	-4	intermediate	0.00738	0.149	396 497 000	2 927 220
0.50	-4	neap	0.00369	-0.4	0	0
0.50	-3	spring	0.00644	0.07	195 902 000	1 262 214
0.50	-3	intermediate	0.01289	-0.4	0	0
0.50	-3	neap	0.00644	-0.4	0	0
0.50	-2	spring	0.00691	-0.4	0	0
0.50	-2	intermediate	0.01383	-0.4	0	0
0.50	-2	neap	0.00691	-0.4	0	0
0.50	-1	spring	0.01148	-0.4	0	0
0.50	-1	intermediate	0.02295	-0.4	0	0
0.50	-1	neap	0.01148	-0.4	0	0
0.50	0	spring	0.00228	-0.4	0	0
0.50	0	intermediate	0.00456	-0.4	0	0
0.50	0	neap	0.00228	-0.4	0	0
0.50	1	spring	0.00275	0.223	638 164 000	1 756 059
0.50	1	intermediate	0.00550	-0.4	0	0
0.50	1	neap	0.00275	-0.4	0	0
0.50	2	spring	0.00228	0.24	701 028 000	1 599 695
0.50	2	intermediate	0.00456	-0.4	0	0
0.50	2	neap	0.00228	-0.4	0	0
0.50	3	spring	0.00369	0.235	682 254 000	2 518 440
0.50	3	intermediate	0.00738	-0.4	0	0
0.50	3	neap	0.00369	-0.4	0	0
0.50	4	spring	0.00826	0.247	727 712 000	6 007 413
0.50	4	intermediate	0.01651	0.162	435 186 000	7 185 101
0.50	4	neap	0.00826	-0.4	0	0
0.50	5	spring	0.01101	0.237	689 735 000	7 591 873
0.50	5	intermediate	0.02201	0.158	423 110 000	9 314 294
0.50	5	neap	0.01101	-0.4	0	0
0.50	6	spring	0.00597	0.243	712 407 000	4 255 406
0.50	6	intermediate	0.01195	0.152	405 283 000	4 841 737
0.50	6	neap	0.00597	0.156	417 130 000	2 491 634

Table G.3: Results from 6 hour spill failure for all storms (h_{setup} = 0.5)

h_{setup} [m]	φ	Tide	Probability	$h_{max,\ canal}$ [m]	Damage costs €	Risk €
1.00	-6	spring	0.00031	-0.4	0	0
1.00	-6	intermediate	0.00063	0.282	868 110 000	544 934
1.00	-6	neap	0.00031	-0.4	0	0
1.00	-5	spring	0.00121	0.223	638 164 000	772 569
1.00	-5	intermediate	0.00242	0.262	786 458 000	1 904 192
1.00	-5	neap	0.00121	-0.4	0	0
1.00	-4	spring	0.00247	0.208	584 974 000	1 442 582
1.00	-4	intermediate	0.00493	0.229	660 038 000	3 255 390
1.00	-4	neap	0.00247	-0.4	0	0
1.00	-3	spring	0.00430	0.181	494 619 000	2 129 038
1.00	-3	intermediate	0.00861	-0.4	0	0
1.00	-3	neap	0.00430	-0.4	0	0
1.00	-2	spring	0.00462	-0.4	0	0
1.00	-2	intermediate	0.00924	-0.4	0	0
1.00	-2	neap	0.00462	-0.4	0	0
1.00	-1	spring	0.00767	-0.4	0	0
1.00	-1	intermediate	0.01533	-0.4	0	0
1.00	-1	neap	0.00767	-0.4	0	0
1.00	0	spring	0.00152	-0.4	0	0
1.00	0	intermediate	0.00305	-0.4	0	0
1.00	0	neap	0.00152	-0.4	0	0
1.00	1	spring	0.00184	-0.4	0	0
1.00	1	intermediate	0.00368	-0.4	0	0
1.00	1	neap	0.00184	-0.4	0	0
1.00	2	spring	0.00152	-0.4	0	0
1.00	2	intermediate	0.00305	-0.4	0	0
1.00	2	neap	0.00152	-0.4	0	0
1.00	3	spring	0.00247	-0.4	0	0
1.00	3	intermediate	0.00493	-0.4	0	0
1.00	3	neap	0.00247	-0.4	0	0
1.00	4	spring	0.00552	-0.4	0	0
1.00	4	intermediate	0.01103	-0.4	0	0
1.00	4	neap	0.00552	-0.4	0	0
1.00	5	spring	0.00735	0.313	1 002 180 000	7 369 380
1.00	5	intermediate	0.01471	-0.4	0	0
1.00	5	neap	0.00735	-0.4	0	0
1.00	6	spring	0.00399	0.344	1 145 370 000	4 570 642
1.00	6	intermediate	0.00798	0.234	678 527 000	5 415 375
1.00	6	neap	0.00399	-0.4	0	0

Table G.4: Results from the 6 hour spill failure for all storms (h_{setup} = 1.00)

h_{setup} [m]	φ	Tide	Probability	$h_{max,\ canal}$ [m]	Damage costs €	Risk €
1.50	-6	spring	0.00018	-0.4	0	0
1.50	-6	intermediate	0.00035	0.325	1 056 530 000	374 038
1.50	-6	neap	0.00018	-0.4	0	0
1.50	-5	spring	0.00068	-0.4	0	0
1.50	-5	intermediate	0.00137	0.343	1 140 610 000	1 557 531
1.50	-5	neap	0.00068	-0.4	0	0
1.50	-4	spring	0.00139	-0.4	0	0
1.50	-4	intermediate	0.00278	0.297	931 842 000	2 592 035
1.50	-4	neap	0.00139	-0.4	0	0
1.50	-3	spring	0.00243	-0.4	0	0
1.50	-3	intermediate	0.00486	-0.4	0	0
1.50	-3	neap	0.00243	-0.4	0	0
1.50	-2	spring	0.00260	-0.4	0	0
1.50	-2	intermediate	0.00521	-0.4	0	0
1.50	-2	neap	0.00260	-0.4	0	0
1.50	-1	spring	0.00432	-0.4	0	0
1.50	-1	intermediate	0.00865	-0.4	0	0
1.50	-1	neap	0.00432	-0.4	0	0
1.50	0	spring	0.00086	-0.4	0	0
1.50	0	intermediate	0.00172	-0.4	0	0
1.50	0	neap	0.00086	-0.4	0	0
1.50	1	spring	0.00104	-0.4	0	0
1.50	1	intermediate	0.00207	-0.4	0	0
1.50	1	neap	0.00104	-0.4	0	0
1.50	2	spring	0.00086	-0.4	0	0
1.50	2	intermediate	0.00172	-0.4	0	0
1.50	2	neap	0.00086	-0.4	0	0
1.50	3	spring	0.00139	-0.4	0	0
1.50	3	intermediate	0.00278	-0.4	0	0
1.50	3	neap	0.00139	-0.4	0	0
1.50	4	spring	0.00311	-0.4	0	0
1.50	4	intermediate	0.00622	-0.4	0	0
1.50	4	neap	0.00311	-0.4	0	0
1.50	5	spring	0.00415	-0.4	0	0
1.50	5	intermediate	0.00829	-0.4	0	0
1.50	5	neap	0.00415	-0.4	0	0
1.50	6	spring	0.00225	0.35	1 174 140 000	2 642 505
1.50	6	intermediate	0.00450	-0.4	0	0
1.50	6	neap	0.00225	-0.4	0	0

Table G.5: Results from the 6 hour spill failure for all storms (h_{setup} = 1.50)

h_{setup} [m]	φ	Tide	Probability	$h_{max,\ canal}$ [m]	Damage costs €	Risk €
2.00	-6	spring	0.00007	-0.4	0	0
2.00	-6	intermediate	0.00013	0.393	1 390 330 000	181 420
2.00	-6	neap	0.00007	-0.4	0	0
2.00	-5	spring	0.00025	-0.4	0	0
2.00	-5	intermediate	0.00050	0.393	1 390 330 000	699 765
2.00	-5	neap	0.00025	-0.4	0	0
2.00	-4	spring	0.00051	-0.4	0	0
2.00	-4	intermediate	0.00103	0.352	1 183 810 000	1 213 710
2.00	-4	neap	0.00051	-0.4	0	0
2.00	-3	spring	0.00089	-0.4	0	0
2.00	-3	intermediate	0.00179	-0.4	0	0
2.00	-3	neap	0.00089	-0.4	0	0
2.00	-2	spring	0.00096	-0.4	0	0
2.00	-2	intermediate	0.00192	-0.4	0	0
2.00	-2	neap	0.00096	-0.4	0	0
2.00	-1	spring	0.00159	-0.4	0	0
2.00	-1	intermediate	0.00319	-0.4	0	0
2.00	-1	neap	0.00159	-0.4	0	0
2.00	0	spring	0.00032	-0.4	0	0
2.00	0	intermediate	0.00063	-0.4	0	0
2.00	0	neap	0.00032	-0.4	0	0
2.00	1	spring	0.00038	-0.4	0	0
2.00	1	intermediate	0.00076	-0.4	0	0
2.00	1	neap	0.00038	-0.4	0	0
2.00	2	spring	0.00032	-0.4	0	0
2.00	2	intermediate	0.00063	-0.4	0	0
2.00	2	neap	0.00032	-0.4	0	0
2.00	3	spring	0.00051	-0.4	0	0
2.00	3	intermediate	0.00103	-0.4	0	0
2.00	3	neap	0.00051	-0.4	0	0
2.00	4	spring	0.00115	-0.4	0	0
2.00	4	intermediate	0.00229	-0.4	0	0
2.00	4	neap	0.00115	-0.4	0	0
2.00	5	spring	0.00153	-0.4	0	0
2.00	5	intermediate	0.00306	-0.4	0	0
2.00	5	neap	0.00153	-0.4	0	0
2.00	6	spring	0.00083	-0.4	0	0
2.00	6	intermediate	0.00166	-0.4	0	0
2.00	6	neap	0.00083	-0.4	0	0
		Total probability:	**0.89**		**Total risk:**	**145 850 000**

Table G.6: Results from the 6 hour spill failure for all storms (h_{setup} = 2.00)

H

Critical Flood Locations

The most critical flood locations along the NSC, ARC and Vecht are determined to indicate where water flows over the quay or levee structure. After this determination a rough estimate for the cost of such a flooding is made. The critical locations for flooding mentioned in Chapter 5 are indicated in Figure H.1.

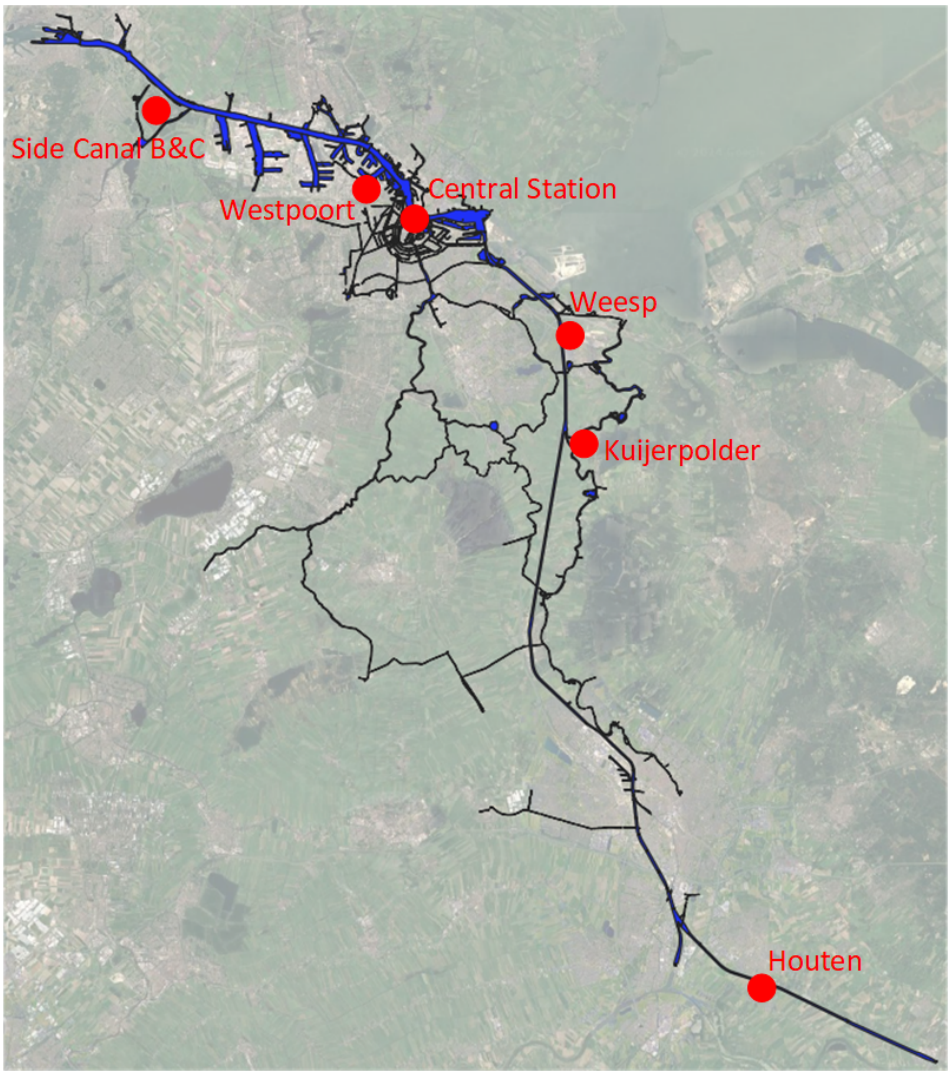

Figure H.1: Critical locations for flooding

Table H.1 summarizes the locations, where the relevant water system and the minimal height of the flooded levee sections are mentioned per location.

Location	Canal\River	Minimal levee section height
Side canals B & C	NSC	+0.40 m NAP
Westpoort	NSC	+0.85 m NAP
Houthavens	NSC	+0.80 m NAP
Central Station Amsterdam	NSC	+0.85 m NAP
Weesp	ARC	+0.65 m NAP
Kuijerpolder	Vecht	+0.35 m NAP
Polder near Houten	ARC	+0.60 m NAP

Table H.1: Critical locations flooding

H.1. Height Maps

Height maps are created with the use of the data from the Dutch elevation database (AHN, 2022). At first a selection for the lowest and therefore most critical flooding locations is made. This is performed for the NSC, ARC and Vecht. Subsequently, height maps of the critical locations are presented.

Side canals B and C are in direct connection with the NSC. Both canals enclose a section of land that is protected by levees, where the lowest levee section is at +0.40 m NAP. Figure H.2 indicates the heights in a map, where the black area represent the heights above the given threshold level. The lowest levee section is indicated with a red circle in the right figure.

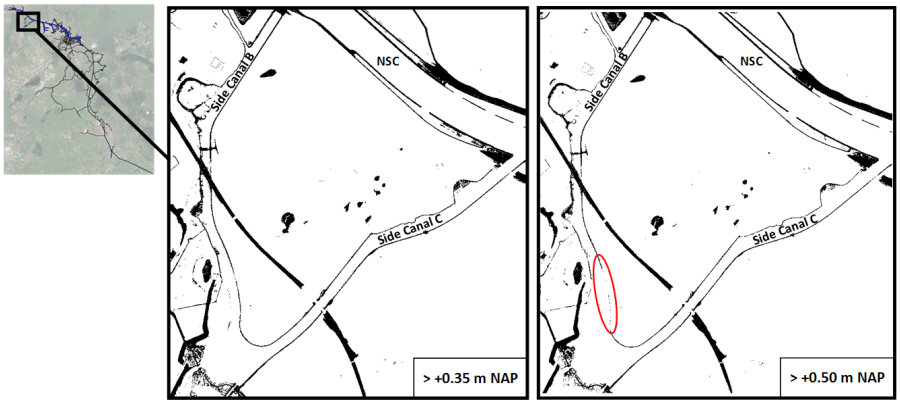

Figure H.2: Height map side canal B & C

Three other locations on the NSC will experience water inflow if the water level rises above +0.80 m NAP. From +0.80 m NAP onward, the buildings in the Houthavens are not protected anymore. Furthermore, the Amsterdam central train station has a quay separating the station from the water at approximately +0.85 m NAP, if water flows into the station, the train traffic might experience nuisance. The third location along the NSC is the Westpoort area, where mostly industry is present. This area can be seen in the height map in Figure H.3. The relationship between the flooding of one of the mentioned areas and the effect on the water levels for the rest of the canal is not studied in this research.

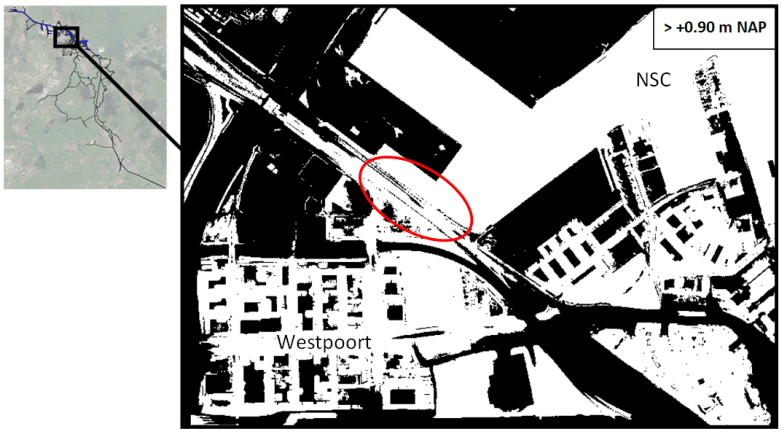

Figure H.3: Height map Westpoort

On the ARC there are two locations prone to flooding, these two locations are at the north of the ARC near Weesp and at the south of the ARC near Houten. The levee sections at Weesp and the polder near Houten are at minimum +0.65 m NAP and +0.60 m NAP respectively. The height maps indicate the sections that are higher than +0.70 m NAP. The difference in the positioning along the ARC does influence the maximum water height in the canal as demonstrated in the results of this research. Further along the ARC, the maximum water levels decrease compared to the start of the ARC. Although the location at Weesp has slightly higher minimum levee height, the location can flood earlier than the location near Houten due to this difference. If one of the areas starts flooding, water is taken out of the canal, which has an effect on the water level along the rest of the canal. Less water in the canal results in lower maximum water levels, however this relation is not studied in detail in this research. The height map for Weesp can be seen in Figure H.4 and for the polder near Houten the height map is presented in Figure H.5.

Figure H.4: Height map Weesp

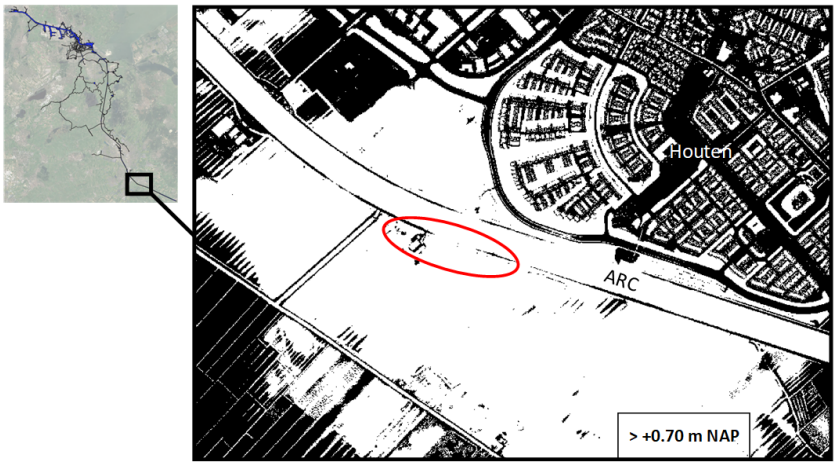

Figure H.5: Height map for the polder near Houten

The last location is present along the Vecht. The Vecht is connected to the ARC, however it is not clear how the water levels of the ARC determine the water levels on the Vecht. The levees along the Vecht are clearly lower than along the ARC and NSC, at the Kuijerpolder the minimal levee height is +0.35 m NAP. The height map for the Kuijerpolder levee can be seen in Figure H.6.

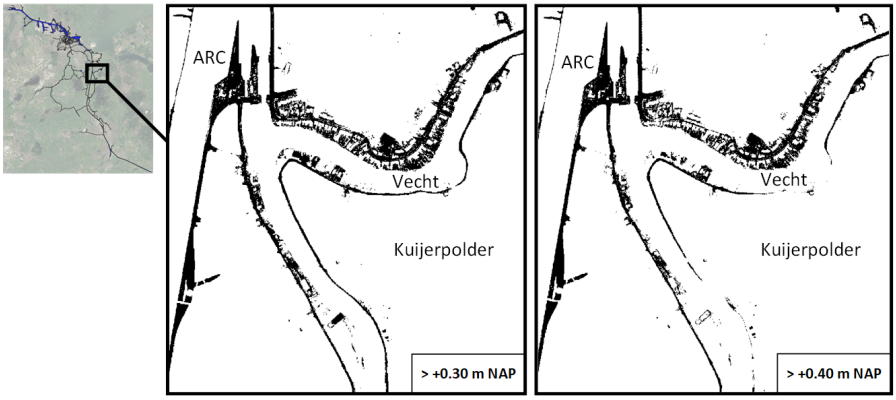

Figure H.6: Height map Kuijerpolder

H.2. Damage Cost of Flooding

The cost of damage in case of water flowing into the area is calculated with the use of a tool developed by Rijkswaterstaat, calculating the cost of damage and if present the number of casualties. The tool is called the SSM (Dutch: Schade en Slachtoffer Module), which translates into damage and casualty module (IPLO, 2024). The water depth in a specific area is the input for the calculator. The module does not incorporate how the water will flow through the area and accumulate in certain areas. For these details according the damages, more research should be done for the different locations.

It is difficult to estimate the volumes that enter the different critical areas. The flood wave has different shapes at different locations and depends on the type of failure and inflow. Furthermore, the levee sections as specified in the height database (AHN, 2022) are locally varying, which makes it difficult to determine the location and the intensity of the overflow. As was already mentioned earlier, the relationship between the floodings is not researched, because inflow in one of the areas leads to lower water levels in the rest of the system. The cost of damages are determined with the use of the SSM for every area. For every area a calculation is performed for 0.01 and 0.1 m of inflow in the full area, the results are summarized in Table H.2.

	Levee height [m NAP]	Water level in area [m]	Area [km^2]	Total inflowing volume [m^3]	Damage	Residents	Casualties
Zijkanaal B en C	+0.40	0.01	4.30	43 000	€ 610 000	229	0
	+0.40	0.10	4.30	430 000	€ 6 000 000	229	0
Houthavens	+0.80	0.01	0.18	1 800	€ 1 300 000	3058	0
	+0.80	0.10	0.18	18 000	€ 13 000 000	3058	0
AMS Central Station	+0.85	0.01	0.07	700	€ 300 000	0	0
	+0.85	0.10	0.07	7 000	€ 3 000 000	0	0
Westpoort	+0.85	0.01	0.90	9 000	€ 3 600 000	76	0
	+0.85	0.10	0.90	90 000	€ 36 000 000	76	0
Weesp	+0.65	0.01	2.70	27 000	€ 8 600 000	11490	0
	+0.65	0.10	2.70	270 000	€ 84 000 000	11490	1
Kuijerpolder	+0.35	0.01	2.40	24 000	€ 730 000	1329	0
	+0.35	0.10	2.40	240 000	€ 7 200 000	1329	0
Houten polder	+0.60	0.01	1.20	12 000	€ 75 000	8	0
	+0.60	0.10	1.20	120 000	€ 740 000	8	0

Table H.2: Damage due to inflow of canal water